Spring 2014

Analysis of a Sponge Bioherm from the Hermosa Group, Molas Lake Area, Colorado

Joanna Hamilton
joannah@bgsu.edu

Analysis of a Sponge Bioherm from the Hermosa Group, Molas Lake Area, Colorado

Joanna Hamilton

Bowling Green State University

Department of Geology

April 2013

Introduction:

The Hermosa Group

The Hermosa Group is a Pennsylvanian (~310 Ma) rock unit found in the southwestern San Juan Mountains and the Paradox Basin. The Paradox Basin is a northwest-southeast trending basin related to the Uncompahgre Uplift in the north, salt deposition and movement throughout, and a Precambrian fault system in the underlying basement rocks (Brown 2002, Trudgill and Arbuckle 2009).

The Uncompahgre Uplift occurred in response to the Ouachita – Marathon Orogeny (related to the Ancestral Rocky Mountains Orogeny) caused by the collision of North America and South America-Africa during the Late Mississippian (~ 320 Ma) (Trudgill and Arbuckle 2009, Pazzaglia et al. 1999). The Paradox Basin formed as a complimentary subsidence basin alongside the uplifted area (Brown 2002). When the basin subsided, smaller structural features formed within it, including step-down grabens close to the uplift and folded areas further away (Baars and Stevenson 1981, Brown 2002). The folded rocks in the basin created topography that was high enough to inhibit circulation within the basin, and mixing of the open marine waters with the saline water already present in the basin during the Pennsylvanian, thereby causing higher salt concentrations in the deeper areas of the basin, near the Uncompahgre Uplift (Baars and Stevenson 1981, Trudgill and Arbuckle 2009).

Salt was deposited in the deeper portions of the basin, along the axis, while carbonate layers were laid down in the less saline waters along the margins of the basin, and sandstone and siltstone layers were deposited beside them (Clark and Stearn 1968, Girdley 1968, Baars and Stevenson 1981). The Uncompahgre stopped uplifting during the Permian (~298 Ma) and the sediments eroded from the Uncompahgre Uplift caused the previously deposited salt to flow through the Paradox Basin along controlled paths created by the underlying Precambrian fault structures (Baars and Stevenson 1981, Trudgill and Arbuckle 2009). The salt continued to flow through the basin until the end of the Jurassic (~145 Ma), when the deposits were finally depleted (Baars and Stevenson 1981).

The Hermosa Group is comprised of the Pinkerton Trail Formation at the base, the Paradox Formation in the middle, and the Honaker Trail Formation at the top (Fig.1) (Baars and Stevenson 1981, Brown 2002).

The Hermosa Formation was first described in 1900 by A. C. Spencer and named for Hermosa Creek in Colorado. Spencer did not indicate a type section and, after two contact revisions and an overview, a composite type section was put together in 1934 by R. I. Roth. In 1954 Wengerd and Strickland limited the name “Hermosa Formation” to indicate all of the carbonate-clastic beds above the Paradox Formation and below the Cutler Formation. In 1958 J. R. Clair revised the definition of the extent of the Hermosa Formation to include the Lime Ridge, Pinkerton Trail, Paradox and Honaker Trail Formations. Wengerd and Matheny further revised the classification by raising the status of the “Hermosa Formation” to the “Hermosa Group” and included as its members the Pinkerton Trail Formation, Paradox Formation and the Honaker Train Formation. The upper contact was revised in 1990, by Loope and colleagues, to its current position (USGS 2014).

The Pinkerton Trail Formation is the oldest member of the Hermosa Group and is comprised of a basal marine siltstone followed by a bed of marine carbonate rocks, and an upper unit composed of thin carbonate beds that have undergone some dolomitization (Brown 2002, Girdley 1968). The mid-unit carbonate rocks contain crinoids, bryozoans, brachiopods, foraminiferans, mollusks, solitary corals, phylloid algae and the sponge, *Chaetetes*, as well as other marine fauna (Brown 2002). When the sea transgressed due, in part, to a deepening of the basin, reefs grew to form barriers and patches in the western portion, causing lagoonal deposits associated with reefs to be deposited as well (Clark and Stearn 1968). The overlying thin carbonate, sandstone and siltstone layers were deposited during the Desmoinesian (~315 Ma) as the Absaroka Sea regressed from the Paradox Basin due to a fall in eustatic sea level (Clark and Stearn 1968). This study focuses on *Chaetetes* fossils from this unit.

The Paradox Formation consists of the aforementioned salt deposits along with interbeds of anhydrite, silty dolomite and black shale – all characteristic deposits of regressive-transgressive sequences (Trudgill and Arbuckle 2009) It is thought that the Paradox Formation, the middle unit of the Hermosa Group, is the result of the repeated emptying and filling of the Paradox Basin, as it demonstrates at least 29 cyclotherms caused by repeated short-lived global sea level rises, and their corresponding falls, related to glaciation episodes on Gondwana (Brown 2002, Girdley 1968, Trudgill and Arbuckle 2009). The evaporitic nature of the basin was brought to an end with a final regression and increased sedimentation, due to the continued rising of the Uncompahgre Uplift (Clarke and Stearn 1968).

The youngest member of the Hermosa Group, the Honaker Trail Formation, consists of clastic sediment eroded from the Uncompahgre Uplift, interbedded with marine black shales and sandy/ cherty limestones, as well as dolomites and siltstones. Fossils found within the Honaker

Trail Formation include foraminiferans, crinoids, gastropods, corals, trilobites, brachiopods and bryozoans (Trudgill and Arbuckle 2009). The Uncompahgre Uplift continued rising throughout the deposition of the Honaker Trail Formation until the increased sediment load added enough sediment into the basin to fill it above sea level (Baars and Stevenson 1981).

Subsequent Tectonic Activity

Throughout the Triassic and Jurassic, the Paradox Basin was largely a tectonically quiet area, however, during the Latest Cretaceous the Laramide Orogeny began (Baars and Stevenson 1981). The Laramide Orogeny reactivated the same Precambrian fault lines that had allowed for the uplift of the Uncompahgre and the formation of the Paradox Basin (Baars and Stevenson 1981, Brown 2002). Due, in part, to the extensive salt deposits within the Paradox Basin, and also to its uplifted position, the basin was left largely undeformed by the Laramide Orogeny and accompanying compressive stresses (Baars and Stevenson 1981). The small amount of deformation acquired during the Laramide Orogeny is almost exclusively related to the enhancement of previously folded features and some of the already-present salt-generated features (Baars and Stevenson 1981).

Following the end of the Laramide Orogeny (~ 40 Ma) the Colorado Plateau was uplifted and tilted (Baars and Stevenson 1981, Brown 2002). Also present on the Colorado Plateau are laccolithic mountains related to volcanism in the San Juan Volcanic Field at the time of the plateau's uplift (Baars and Stevenson 1981, Brown 2002). At least four of the laccolithic mountains present on the plateau have been dated to between 61 and 84 Ma – during the Laramide Orogeny. The other laccoliths have been dated to ~24 – 48 Ma (Latest Oligocene – Early Eocene), when the San Juan Volcanic Field was active (Baars and Stevenson 1981, Gilbert 2012). The volcanic activity in the area that led to the injection of laccoliths also created sills,

dikes and stocks, as well as hydrothermal activity throughout the plateau t altered portions of the Paleozoic bedrock (Baars and Stevenson 1981). The tilting of the plateau also caused rapid erosion and down cutting by rivers through the salt-flow deposits, thereby creating collapsed structures by groundwater and surface water solution within the Paradox Basin (Baars and Stevenson 1981). Subsequent glacial activity in North America left glacial outwash deposits, stream alluvium and alluvial fan deposits in the area.

Pennsylvanian Climate of North America

By the end of the Mississippian sea level had dropped to levels similar to those of today, but with the beginning of the Pennsylvanian, sea level was on the rise again (Haq and Schutter 2008). Throughout the Pennsylvanian sea level fluctuated dramatically due, in part, to the formation of Pangea (Latest Mississippian) and the repeated glaciation of Gondwana (Brown 2002, Haq and Schutter 2008). During the Pennsylvanian, North America was located near the equator and rotated so that, what is currently Utah, was the northern tip of the continent and present-day New Jersey would have been near the southern tip (Brown 2002).

On the eastern side of North America coal swamps were forming, while the western side of the continent was experiencing a more arid climate, though it was mostly covered over by a shallow sea (Brown 2002, Nagarajan 2012). In the west, sandwiched between the open ocean and the interior seaway, sat uplifted lands in the present-day Four Corners region, while in the east the Appalachian Highlands created a barrier between the coal swamps and the sea (Brown 2002, Heckel 2008).

During the Pennsylvanian atmospheric CO_2 concentration levels were slightly higher than today's, and oxygen concentrations also increased from Mississippian levels (Dudley 1998).

Anthropogenic Climate Change

Humans have had an impact on the Earth since they evolved. While many people are concerned about these effects it is unknown whether the impacts that humans have on the Earth will be represented in the geologic record as anything more than a thin line in a stratigraphic section. The term "Anthropocene" is being used in the geological literature to distinguish the present time, affected by environmental changes caused by humans, from previous time periods that experienced naturally-occurring environmental changes over time (Kolbert 2011, Zalasiewicz et al. 2010). The planet has been subjected to such distinct changes in biota, chemical introductions and sedimentary changes since the Industrial Revolution that some believe there is sufficient evidence to create a Holocene-Anthropocene boundary at this time (Zalasiewicz et al. 2008).

Today, as atmospheric CO_2 concentrations rise and oceans become more acidic, coral reefs are in particular danger from the threat of ocean surface temperature changes and ocean chemistry changes. Also threatening the existence of coral reefs is the rise in eustatic sea level caused by the melting of the polar ice caps.

Reefs

A reef is often defined as a discrete carbonate structure, formed or bound by in-situ organic components, that develops topographic relief on the sea floor (Wood 2000). Many factors influence reef growth and production including, but not limited to, temperature, light penetration below the water surface, turbidity (and lack thereof), sedimentation rates, space, and $CaCO_3$ availability in the water (Tasch 1973). Once reefs are established they can affect water and sediment flow within an area, causing back-reef and lagoonal environments to form as well, while simultaneously preventing coastal erosion and creating protected harbors (Tasch 1973,

Wood 1998). Bioherms have the same effects on the surrounding environment, but a bioherm is a small, lens-shaped buildup of biogenic carbonate, often found in patches and mounds, rather than a continuous reef.

Reef organisms belong to guilds. A guild is a group of organisms that play a specific role within a reef environment. Organisms can belong to one of five guilds: constructors, binders, bafflers, destroyers or dwellers. Constructors provide the main structural framework for the reef and can be overgrown by binders (algae, foraminiferans, etc.), which contribute to the stability of the reef. Bafflers interrupt the flow of water around/ across the reef, promoting deposition of sediment, and dwellers are just inhabitants that add diversity to the reef environment. Destroyers, including grazers and boring organisms, break down the main framework of the reef, converting it to fine-grained carbonate sediment (Morelock et al. 2005). Fine-grained carbonate sediment can then be overgrown by binders, again, and cemented in place

The dominant organisms that create reefs and bioherms are influenced by the abundance of calcite versus aragonite in the sea water. As oceans become more acidic due to an increase in dissolved-CO_2, and surface water temperatures increase, growth of calcitic builders, like sponges, rather than aragonitic builders, like scleractinian corals, is promoted (Wood 1998). This is evidenced by the fact that when modern coral reefs become stressed, due to environmental changes, sponges and algae tend to encrust modern reefs because they are better suited for the new environment (Wood 1998).

Chaetetes

Chaetetes is a demosponge that lived across the globe from the Middle Devonian to the Permian. *Chaetetes* was first described and identified in 1829 by Fischer von Waldheim and was classified as a tabulate coral due to the presence of tabulae (sub-horizontal to funnel-shaped

floors) and aseptate corallites (Hill and Stumm 1956). The interpretation of *Chaetetes* as a tabulate coral was supported by Milne-Edwards and Haime in 1850 and Lane and Martin in 1966. It was also considered to be a calcareous algae by Sokolov in 1962, and a bryozoan by Nicholson in 1847. It was suggested that C*haetetes* be reclassified from Cnidaria to Porifera by Kirkpatrick in 1909. Supporters of the move to Porifera cited the lack of "true" septa, asexual reproduction, and homomorphy with recent sclerosponges as evidence for the change. The inconsistencies [lack of spicules and astrorhizae] cited by objectors to this move, have since been resolved and *Chaetetes* has been moved from Sclerospongiae to Demospongiae, as Sclerospongiae is now thought to be a sub-category under Demospongiae (Connolly et al. 1989).

During the Pennsylvanian, from the Morrowan to the Desmoinesian, *Chaetetes* was known to form bioherms on which crinoids, algae, ostracods, foraminiferans, brachiopods, and mollusks are also found (Connolly et al. 1989). *Chaetetes* were often tossed around by wave action in very shallow water or areas with medium – high energy, until they reached a critical size and were able to withstand the force of the waves (Connolly et al. 1989). However, multiple growth directions within a single *Chaetetes* could also be indicative of deeper water with occasional storm activity producing waves strong enough to topple the sponges (Brown 2002). Chaetetid bioherms have often been found in association with algal (especially the phylloid alga *Ivanovia*) mounds and mats – though others have been found in smaller, isolated buildups that had ceased to be productive and were subsequently encrusted by the aforementioned organisms (Connolly et al. 1989, Wahlman 2002). It has been suggested that the majority of chaetetid bioherms grew in enclosed, near-intertidal locations, while some may have grown in open shelf environments below wave base (Connolly et al. 1989).

The majority of *Chaetetes* found in the Pinkerton Trail Formation are preserved in growth position, suggesting that the matrix was deposited *in situ* by biological processes, and that *Chaetetes* acted as a constructor within the bioherm (Girdley 1968, Morelock et al. 2005). The lack of winnowing of the matrix material, as well as the excellent preservation of the sponges, suggests that no strong wave action was present where the bioherms grew, indicating a low-energy environment (Brown 2002, Girdley 1968). The noticeable decline in sponge fossils within the upper foot of the marine carbonate rocks indicate that sedimentation rates increased to such a rapid rate of deposition that the bioherms were buried more quickly than they could grow (Girdley 1968).

Research Importance and Questions

The study of sponge bioherms is important because understanding the environments in which they lived can help to determine the ecological parameters in which they may be found in the future. Modern reefs are composed of scleractinian corals, but with ocean chemistry and global climate changing, sponges may become the dominant reef builders again. The information gathered in this study can also be used to model reef responses to climate change and to help understand complex stratigraphic sequences, such as the Hermosa Formation.

Chaetetes sponges from the Pinkerton Trail Formation were investigated in this study. The questions addressed in this analysis include: What might growth habits of the sponges indicate about the environment in which they were growing? Is there evidence of encrusting growth of other organisms? Is there evidence for the association of photosynthetic organisms with the sponges? What do the associated organisms tell us about the environment in which the sponges were growing?

Methods:

Samples have been chosen from roughly equivalent horizons in the Pinkerton Trail Formation at two localities: Molas Lake (Main Fossil Site) and Andrews Lake (Fig. 2). These beds contain extensive *Chaetetes* fossils, and are immediately overlain by a sandstone unit showing evidence of tidal currents, suggesting a shallowing-up cycle (M. M. Yacobucci, personal communication, April 1, 2014). These beds were chosen due to previous use by other scientists and documentation of possible fossil finds. Due to the variety of available specimens, two hand samples were chosen from the Andrews Lake site, while four were chosen from the Molas Lake site. The Molas Lake hand samples were chosen either because there were multiple sponges present in the hand sample or because of the good quality of preservation of a single sponge (Fig. 3). After observation with a hand lens and the determination of where the most useful information might be acquired from the samples, they were cut using a rock saw.

After the samples were cut down to the appropriate sizes they were mounted onto slides. Due to the soft nature of these carbonate rocks, and the veining through them (from Cenozoic hydrothermal activity), some of the samples broke during cutting and needed to be glued back together before they were mounted onto the slides. The samples were then cut and ground down using a Logitech Automated Thin Section Machine.

The thin sections were photographed using a digital camera and a petrographic microscope at magnifications of 25x, 100x and 250x. Photographs included images of the matrix material, the sponges, the sponge-matrix boundary, and, when present, veins and sponge-vein boundaries. The thin sections were photographed under plain-polarized light.

The hand samples that remained were polished on a lap wheel with grit up to 600 microns. Due to the soft nature and veining/fracturing of these rocks, parts of the samples

chipped away and held grit during polishing, thereby scratching the surface of the samples and making them very difficult to polish evenly.

Eighteen thin sections were made from six hand samples. One sample from the Andrews Lake site produced one thin section, while the other produced two. The Molas Lake Site fossils were made into varying numbers of thin sections based on what was visible on the hand samples. Larger hand samples were allotted more thin sections. If multiple sponges were present in one hand sample, each sponge was represented by at least one thin section. For each thin section, lithology and grain size were determined. Also documented are fossils, as well as syn- and post-depositional structures. Correlation of microstructures to macrostructures was done with hand samples. For more detailed information on the thin sections and hand samples, refer to the Appendix, which also includes images for each thin section and hand sample.

Results:

Sedimentology:

The samples used in this study have been classified here as framestones. In all of the thin sections crinoid fragments are abundant, as are foraminiferans, and brachiopod and mollusk shell fragments (Fig. 4). Sponge fragments are also present in the matrix material (Fig. 5), as well as occasional ostracode shells (Fig. 6). Also present are rip-up (Fig. 7) and curl-up clasts (Fig. 4). Due to the size and abundance of fossil fragments, as well as the presence of micrite, rather than sparry calcite cement, the matrix was determined to be a biomicrite (Fig.4).

Recrystallization of fossil fragments by sparry calcite was observed throughout both the Molas Lake and Andrews Lake samples (Figure 8). The veining present throughout the samples was determined to be calcite as well, due to effervescence and twinning within the crystals.

On many of the boundaries between the sponge and biomicrite, iron staining is present. Iron staining is also present along some of the recrystallization-biomicrite boundaries. Within some of the sponge samples there is also iron staining along the edges of the internal chambers and along the edges of vein-biomicrite boundaries (Fig. 9).

Chaetetes:

The sponges present in the thin sections were determined to be *Chaetetes* due to the polygonal walls separated by tabulae. Also supporting this analysis is the lack of septa within the polygonal cavities (Fig. 10) and the encrusting growth of phylloid algae on the sponge's surface, in at least one instance. (Fig. 11)

Sponge Growth Habits:

When viewed from the base, hand sample T1.1a, from the Andrews Lake site, shows two distinct growth directions. The first growth direction, at the center of the sample, appears to indicate that the sample was turned at least once, a minimum of 90^{o}, and then grew vertically, until it died (Fig. 12). Thin section B1.1b1, from the Molas Lake site, also shows multiple growth directions, indicating a similar sequence of events (Fig. 13).

Hand sample B6, from the Molas Lake site, shows a 3-dimensional view of one large sponge's growth (see Appendix).

Associated Organisms:

Crinoid fragments were recognized by their characteristic appearance, a disc with a central cavity (similar to a bagel) as well as by the growth rings present on chipped fragments (Fig. 7 and Fig. 13). Ostracod shell fragments were recognized by their characteristic "jelly-bean" shape (Fig. 6). Brachiopod and mollusk shell fragments were identified based on the tapered ends of shell fragments as well as by the slight angle of the shells. Efforts to

differentiate brachiopod and mollusk shells proved fruitless, as no distinguishing characteristics could be identified. Foraminiferans were identified by their chambered appearance and the spirals of the fusilinids (Fig. 7). Cyanobacterial associations were determined by the presence of walled calcispheres (Fig. 10). Phylloid algal associations were identified by the curved disk, similar to a potato-chip, texture and associated void space infilled with sparry calcite (Fig. 11 and Fig. 14).

Evidence for Ecological Interactions:

Thin section B1.1a2 shows two sponges growing against each other, possibly competing for space in the bioherm (Fig. 15). Walled calcispheres indicate the presence of cyanobacteria growing on the sponges (Fig. 10). Phylloid algae is also present in these samples and appears to have grown on portions of the sponges as well (Fig. 11 and Fig. 14).

Discussion:

Rip-up clasts indicate that the substrate was cemented before wave action became strong enough to move it again. Curl-up clasts indicate partially cemented substrate, rather than wholly cemented substrate. Multiple growth directions on only a few samples along with the presence of the rip-up and curl-up clasts in the same samples, indicates that rotational growth and substrate alteration were caused by storm-weather wave action, rather than fair-weather wave action. This evidence, along with the presence of fusilinid foraminiferans, crinoid fragments, brachiopod and mollusk shell fragments, suggests that the bioherm grew above storm-weather wave base in shallow water with low to moderate wave energy. It also suggests that many of the samples used in this study may have been located in protected areas of the bioherm because only storm-weather wave energy appeared to affect their growth habits. The presence of complete bivalve shells, foraminiferans, interpreted space competition, phylloid algae and walled

calcispheres also indicate that the sponges grew in a closely-spaced, protected environment within the bioherm.

The extensive veining and recrystallization throughout both samples is most likely related to the hydrothermal activity of the San Juan Volcanic Field. The iron staining along the sponge-biomicrite/ veining-biomicrite boundaries may be related to this as well. The hydrothermal activity may have left behind iron particulates that were later oxidized and stained the rocks and fossils. The observed affinity of phylloid algae, cyanobacteria, and *Chaetetes* (Pratt 1984, Wahlman 2002, Grammer and Ritter 2009, Connolly et al. 1989, Corrochono and West 2013) might suggest that the iron staining reflects alteration of algal organic matter; however, the presence of walled calcispheres without iron staining and phylloid algal fossils suggests that the iron staining is simply the result of hydrothermal activity, and not alteration of fossilized organic material within the samples.

There is no evidence that imposition of matrix materials affected the growth direction or morphology of the sponges. There is however, evidence that sponges influenced the growth of other sponges by growing into and around each other in closely-packed spaces, as evidenced by the aforementioned interpreted space competition.

The minimal geographic variability shown by the samples that were analyzed indicates that there were slight environmental differences between these contemporaneous fossil sites. However, the overall average height of the sponges – approximately 8.6 cm – also suggests that there was a similar growth control on their height across the area. The tallest sponge however, 20.2 cm, suggests a maximum growth height of just above 20 cm throughout the area. This constraint suggests that, while growth rates were not equal, there was perhaps a cut off above 20 cm due to the shallow depth of the water

Conclusion:

The observations of hand samples and thin sections allow the interpretation of the depositional environment for these sponge-rich horizons of the Pinkerton Trail Formation of the Hermosa Group. The average height of 8.6 cm suggests that there was a uniform growth rate across the bioherm. The rotational growth of samples from both the Molas Lake and Andrews Lake areas suggest that there was also a uniform wave energy throughout, indicating that there was similar topography around both areas, and that similar wave action affected both sites as well. Encrusting growth of phylloid algae, along with the presence of walled calcispheres indicate an environment shallow enough for photosynthetic organisms and foraminiferan's prey to flourish alongside the sponges.

The environment in which these chaetetid bioherms were situated changed dramatically as the Absaroka Sea regressed, the Uncompahgre Uplift continued uplifting, and sediment load increased, though evidence of this was not observed within these samples from a single time slice of the Hermosa Group. The change in environment that led to the demise of these *Chaetetes* is similar to that facing coral reefs today. Throughout geologic time we see that the dominant reef constructor is often the most at-risk member of the reef community. However, the difference today is that sponges are overgrowing and outcompeting the modern scleractinian corals, and are on their way to becoming the dominant constructors of the future. Hopefully the research presented in this paper can be of use to reef-response modelers and environmentalists who wish to help the current reef ecosystems cope with, and adjust to, anthropogenic climate change today.

Acknowledgements

Special thanks to Dr. Margaret Yacobucci for providing the sponge specimens used in this study, and also for her suggested revisions and edits. Thanks to Dr. Jeffery Snyder for advising on this project. Last, but not least, thanks also to Dr. Charles Onasch for assisting with the preparation of thin sections and polished hand samples.

References

Baars, D. L. and Stevenson, G. M. 1981. Tectonic evolution of the Paradox Basin, Utah & Colorado. In D. L. Wiegand (Ed.), *Geology of the Paradox Basin: 1981 Field Conference*. Rocky Mountain Association of Geologists; Denver. Pp. 23 – 31.

Brown, A. L. 2002. Outcrop to subsurface stratigraphy of the Pennsylvanian Hermosa Group southern Paradox Basin. *Unpublished dissertation*. Louisiana State University and Agricultural and Mechanical College.

Clark, T. H., and Stearn, C. W. 1968. *Geological Evolution of North America*. 2 ed., pp 188 – 192. New York: The Ronald Press Company.

Connolly, W. M., Lambert, L. L., and Stanton Jr., R. J. 1989. Paleoecology of Lower and Middle Pennsylvanian (Middle Carboniferous) *Chaetetes* in North America. *Facies*. 20. 1; 139 – 168.

Corrochano, Diego and West, Ronald R. 2013. A new plate-like hypercalcified chaetetid demosponge (*Loiscupula bachendensi* gen. nov. sp. nov) from the Cantabrian Zone (Moscovian, Pennsylvanian, NW Spain), *Palaeontologia Electronica*. 16. 2; 18A; 18p.

Dudley, R. 1998. Atmospheric oxygen, giant Paleozoic insects and the evolution of aerial locomotor performance. *The Journal of Experimental Biology*. 201; 1043 – 1050.

Gilbert, H. 2012. Crustal structure and signatures of recent tectonism as influenced by ancient terranes in the western United States. *Geosphere*. 8; 141 – 157. Doi: 10.1130/GES00720.1

Girdley, W. A. 1968. Character of part of the Hermosa Formation (Pennsylvanian), San Juan Mountains, Colorado. In J. Shoemaker (Ed.), *Guidebook of San Juan – San Miguel – La*

Plata Region, New Mexico and Colorado. 19 ed. New Mexico Geological Society. pp. 150 - 158

Grammer, G. M. and Ritter, A. L. 2009. Phylloid algal mounds in the paradox basin, southwestern U.S.A. – an alternative to the in situ constructional growth model?. In P. K. Swart, Eberli, G., and McKenzie, J. (Eds.), *IAS Special Publication: Perspectives in Carbonate Geology*; Issue 41. Wiley - Blackwell.

Haq, B. U. and Schutter, S. R. 2008. A chronology of Paleozoic sea-level changes. *Science*. 322; 64–68.

Heckel, P.H. 2008. "Pennsylvanian cyclothems in Midcontinent North America as far-field effects of waxing and waning of Gondwana ice sheets". *Resolving the late Paleozoic ice age in time and space: Geological Society of America Special Paper*. 441; 275–289.

Hill, D. and Stumm, E. C. 1956. Tabulata. In R. C. Moore (Ed.), *Treatise on Invertebrate Paleontology Part F: Coelenterata* 1 ed., pp. 444 – 449, 454 - 456. Lawrence: University of Kansas Press and The Geological Society of America.

Kolbert, E. 2011, March. Age of man. *National Geographic*.

Lane, N. G. and Martin, R. A. 1966. Redescription of *Chaetetes milleporaceus* Milne-Edwards & Haime, 1851. *Journal of Paleontology*. 40. 3; 651 – 654.

Morelock, J., Ramirez, W., Hallock, P. and D. Hubbard. (2005). *Coral biology and reef development*. http://geology.uprm.edu/Morelock/biolog.htm

Nagarajan, R. V. 2012. A critique on the evolution of landscape architecture & creation of landscape evolution model, in A. Chang and T. Yingthawornsuk (Eds.), *International Conference on Civil and Architectural Applications (ICCAA'2012)* pp. 79 – 83. Phuket, Thailand.

Pazzaglia, F. J., Woodward, L. A., Lucas, S. G., Anderson, O. J., Wegmann, K. W., and Estep, J W. 1999 Phanerozoic geologic evolution of the Albuquerque area. In *New Mexico Geological Society Guidebook, 50th Field Conference*, Albuquerque

Pratt, B. R. 1984. *Epiphyton* and *Renalcis* – diagenetic microfossils from the calcification of coccoid blue-green algae. *Journal of Sedimentary Petrology*. 54. 3; 948 – 971.

Tasch, P. 1973. *Paleobiology of the Invertebrates*. 1 ed., pp 172 – 186. New York: John Wiley & Sons.

Trudgill, B. D. and Arbuckle, W. C. 2009. Reservoir characterization of clastic cycle sequences in the Paradox Formation of the Hermosa Group, Paradox Basin, Utah. Utah Department of Natural Resources.

USGS. 2014. Hermosa group. URL: http://3dparks.wr.usgs.gov/coloradoplateau/lexicon/hermosa_group.htm

Wahlman, G. P. 2002. Upper Carboniferous – lower Permian (Bashkirian – Kungurian) mounds and reefs. In *SEPM Special Publication: Phanerozoic Reef Patterns*. 72; 271 – 338. Society for Sedimentary Geology.

Walker, J.D., Geissman, J.W., Bowring, S.A., and Babcock, L.E., compilers. 2012. Geologic time scale v. 4.0. Geological Society of America. doi: 10.1130/2012.CTS004R3C.

Wood, R. 1998. The ecological evolution of reefs. *Annual Review of Ecological Systems*. 29; 179 – 206.

Wood, R. 2001. Are reefs and mud mounds really so different? *Sedimentary Geology*. 145; 161 – 171.

Zalasiewicz, J., Williams, M., Smith, A., Barry, T., Coe, A., Brown, P., Cantrill, D., Gale, A., Gibbard, P., Gregory, F., Hounslow, M., Kerr, A., Pearson, P., Knox, R., Powell, J.,

Waters, C., Marshall, J., Oates, M., Rawson, P., and Stone. P. 2008. Are we now living in the anthropocene?. *GSA Today*. 18, 2; 4.

Zalasiewicz, J., Williams, M., Steffen, W., & Crutzen, P. 2010. The new world of the anthropocene. *Environmental Science and Technology*. 44; 228-2231.

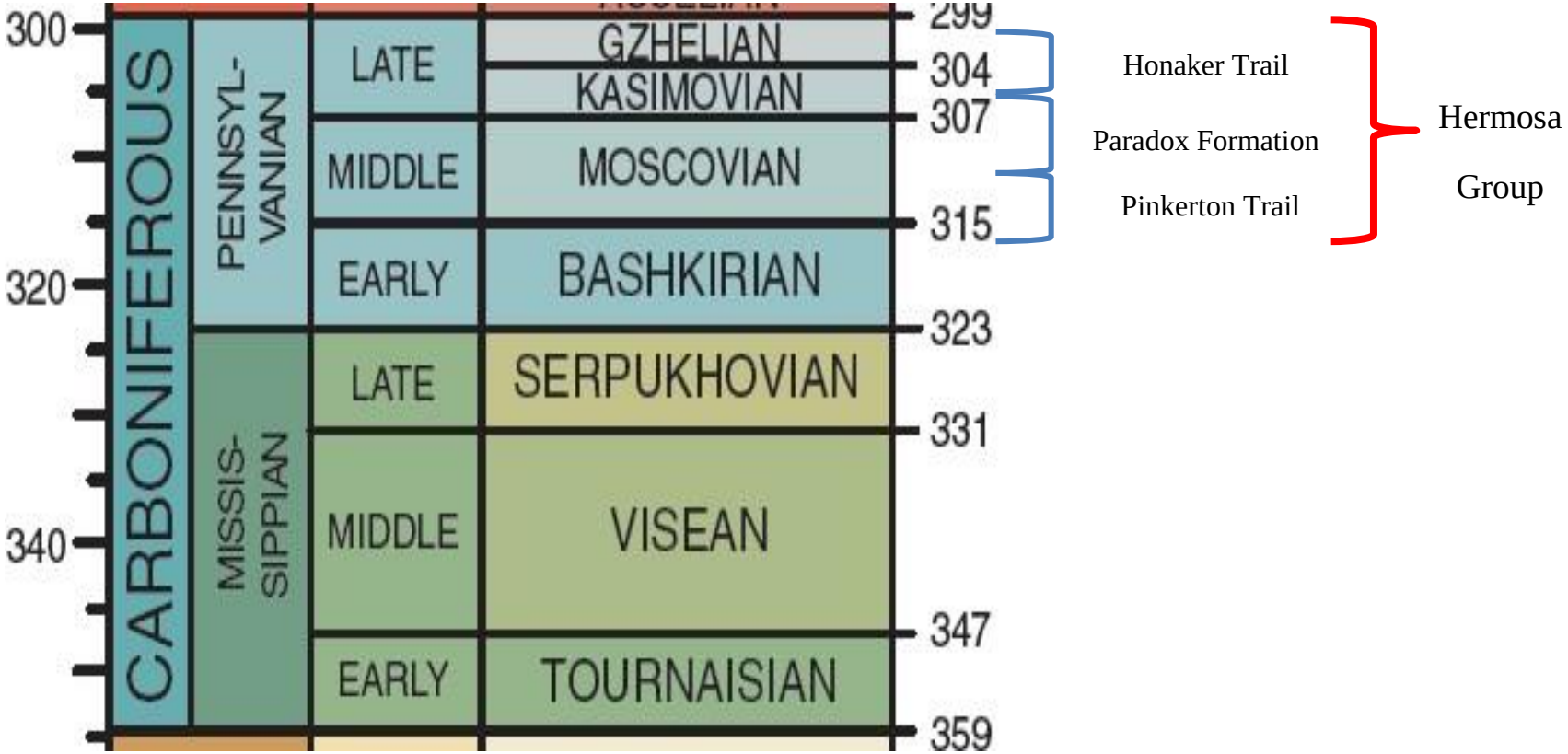

Figure 1. Geologic time scale modified to show time span of the Hermosa Group (Walker et al. 2012)

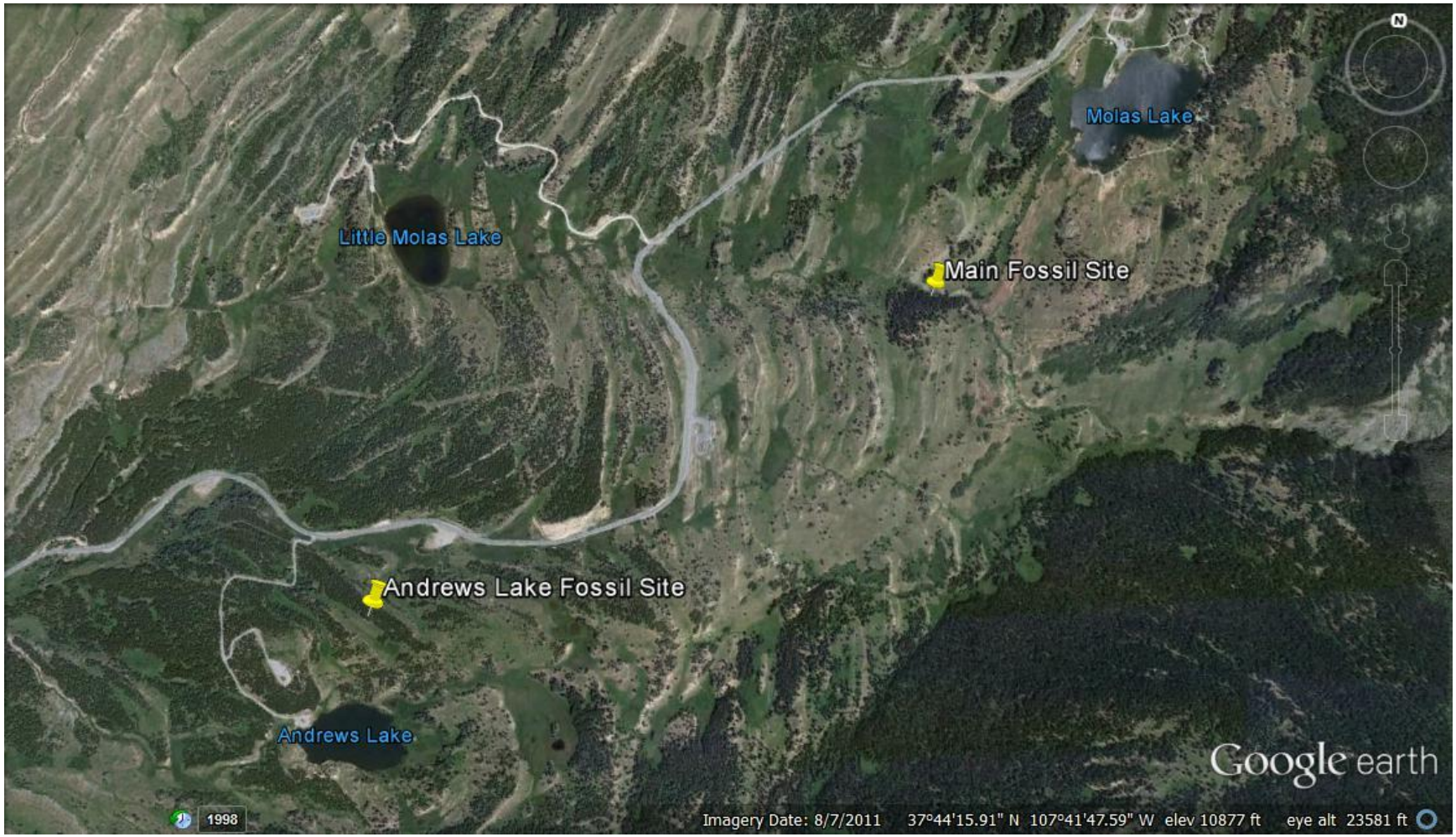

Figure 2. Sample locations (from GoogleEarth).

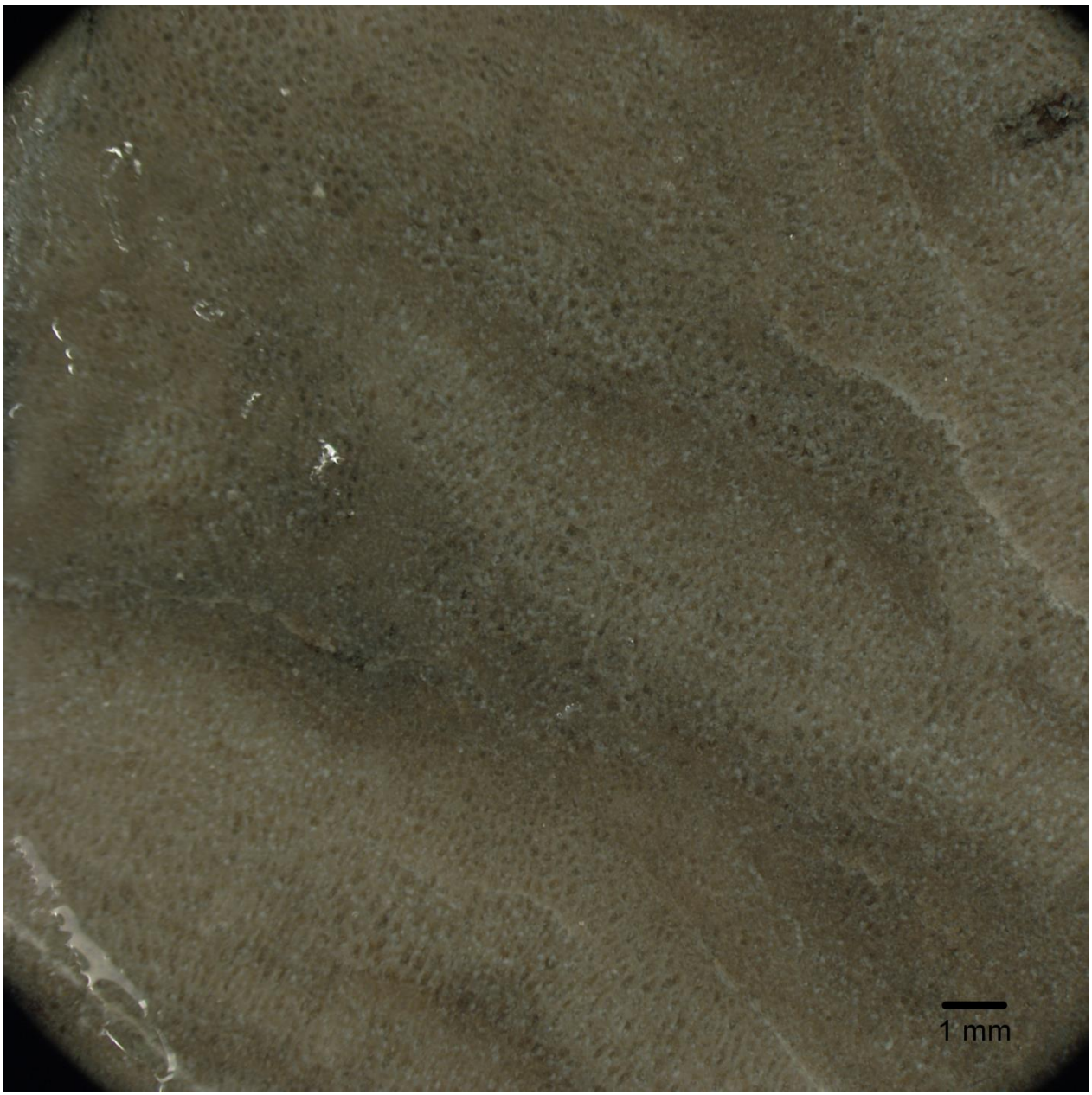

Figure 3. Hand sample T1.1 showing the internal structure of *Chaetetes*. Scale: 1mm.

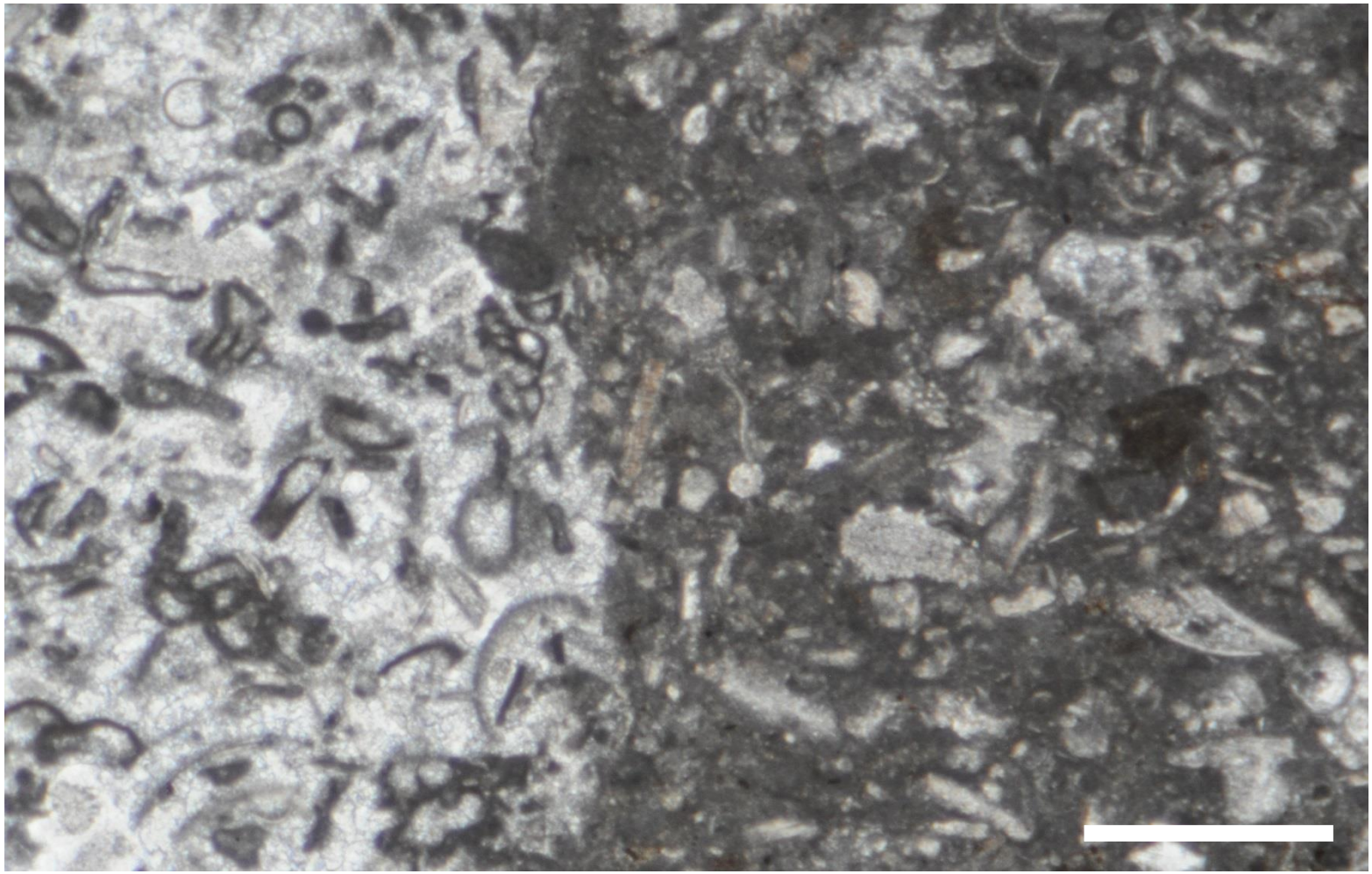

Figure 4. Thin section B6.4b made from a Molas Lake sample showing a curl-up clast boundary (the darker biomicrite). Shell fragments, foraminiferans and crinoid fragments can be seen within the curl-up and within the regularly deposited sediment. That the clasts curled-up rather than ripped-up here, indicates that the substrate was relatively hard, but not cemented, prior to this deformation. Scale: 1mm.

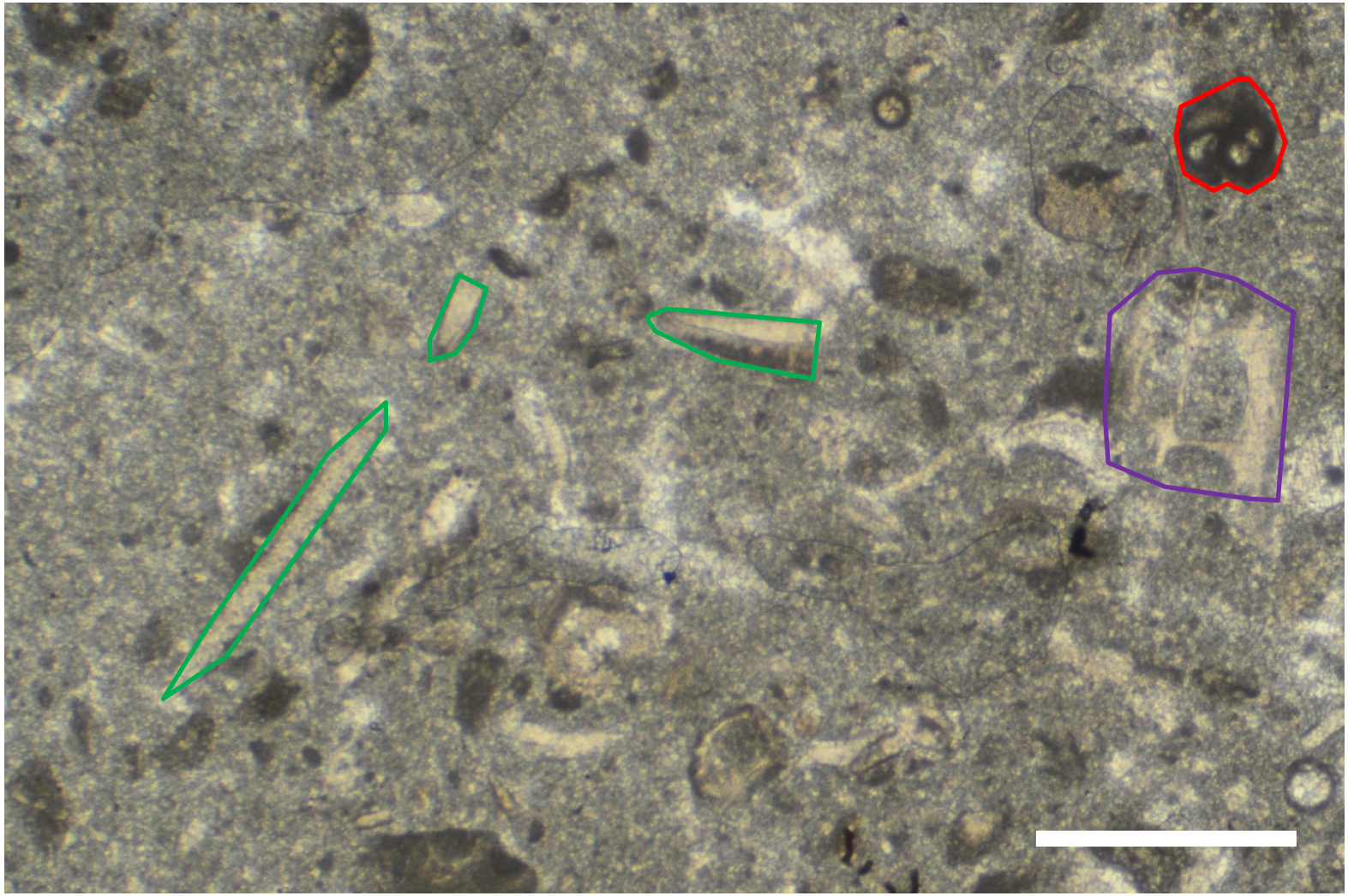

Figure 5. Thin section B1.1b1 showing shell fragments (outlined in green), a foraminiferan (outlined in red), and a sponge fragment (outlined in purple) in the biomicrite matrix. Scale: 1mm.

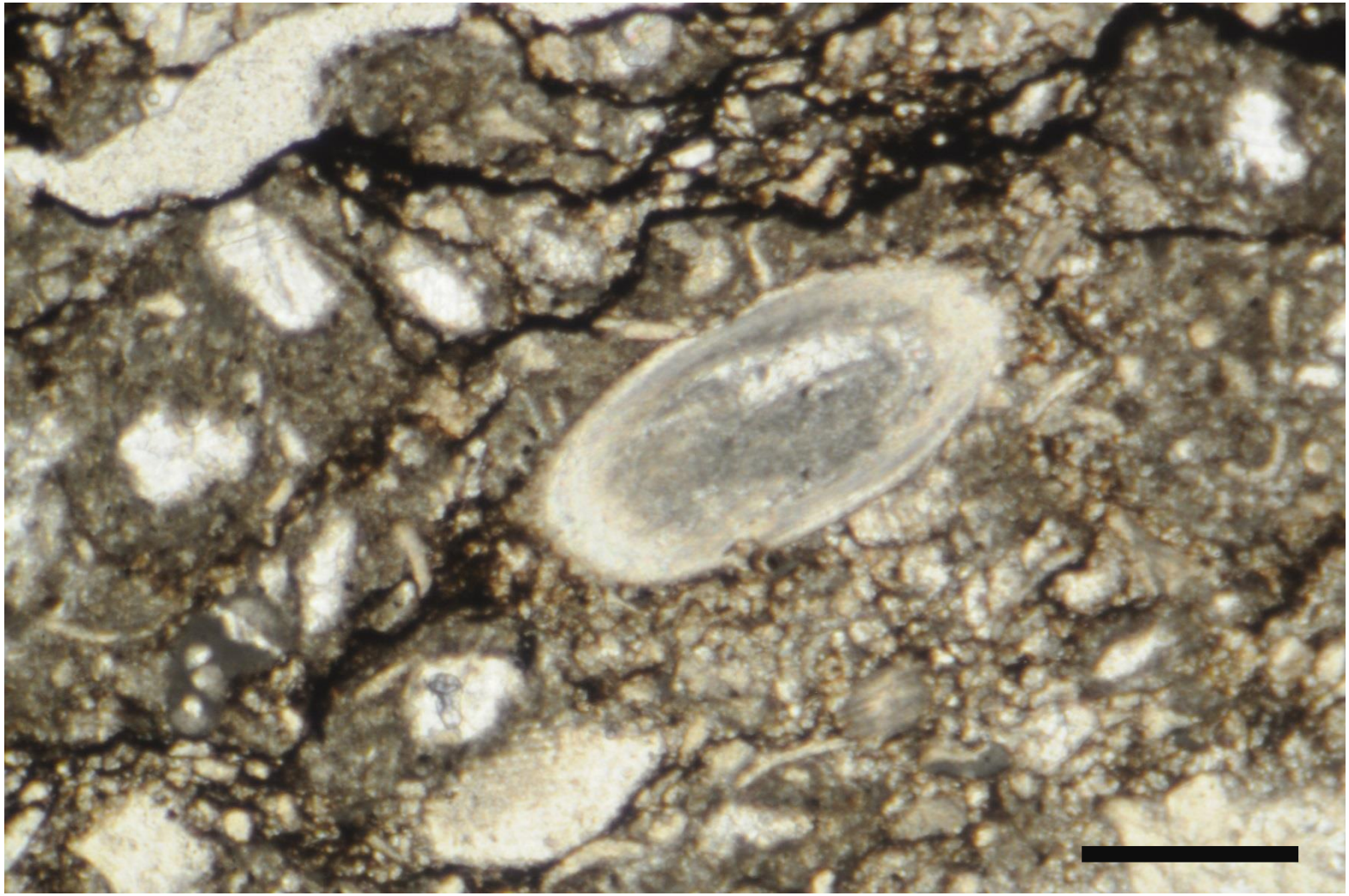

Figure 6. Thin section T1.1a showing an ostracod shell (center) in biomicrite. Scale: 1mm

Figure 7. Thin Section B1.1b1 showing rip-up clasts (outlined in orange) as well as a shell fragment (outlined in green), crinoid stem fragments (outlined in blue) and a foraminifera (outlined in red) that have been recrystallized by sparry calcite. Scale: 1mm.

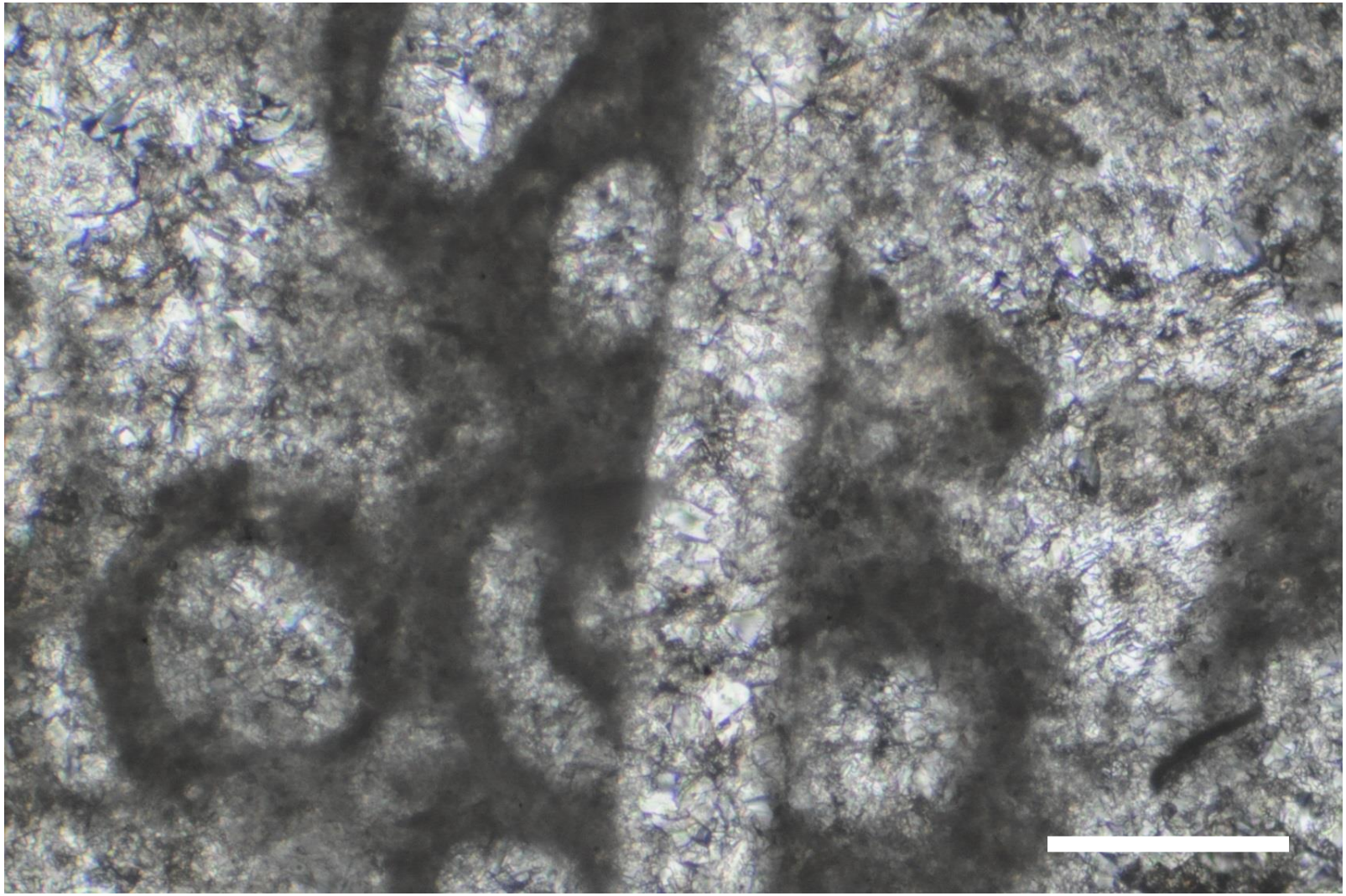

Figure 8. Thin section B6.2e showing sparry calcite recrystallization of a shell fragment (center) and foraminiferans (around the shell fragment). Scale: 0.15 mm

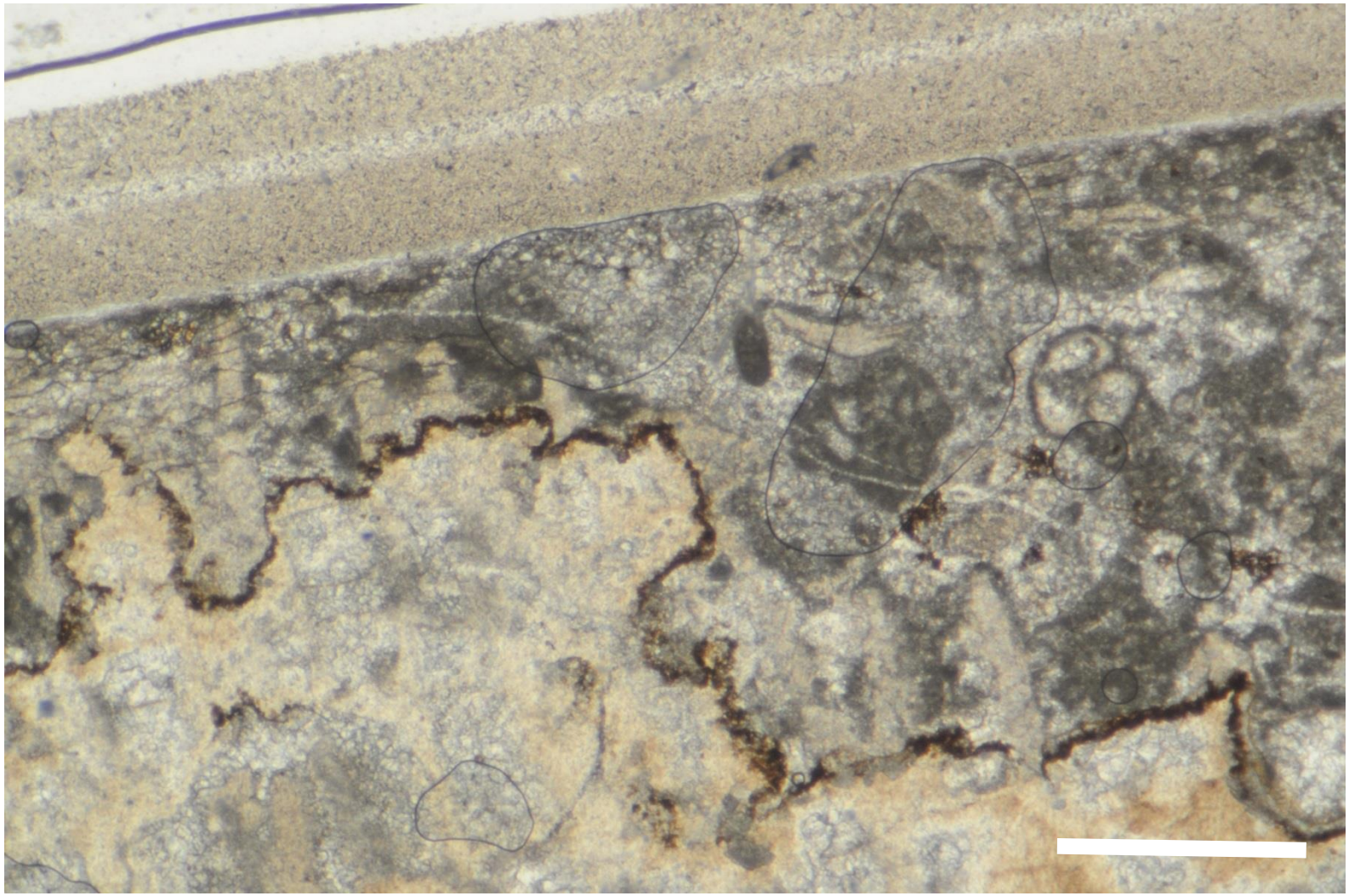

Figure 9. Thin section B1.1b2 showing iron staining along the sponge-biomicrite boundary. Scale: 1mm.

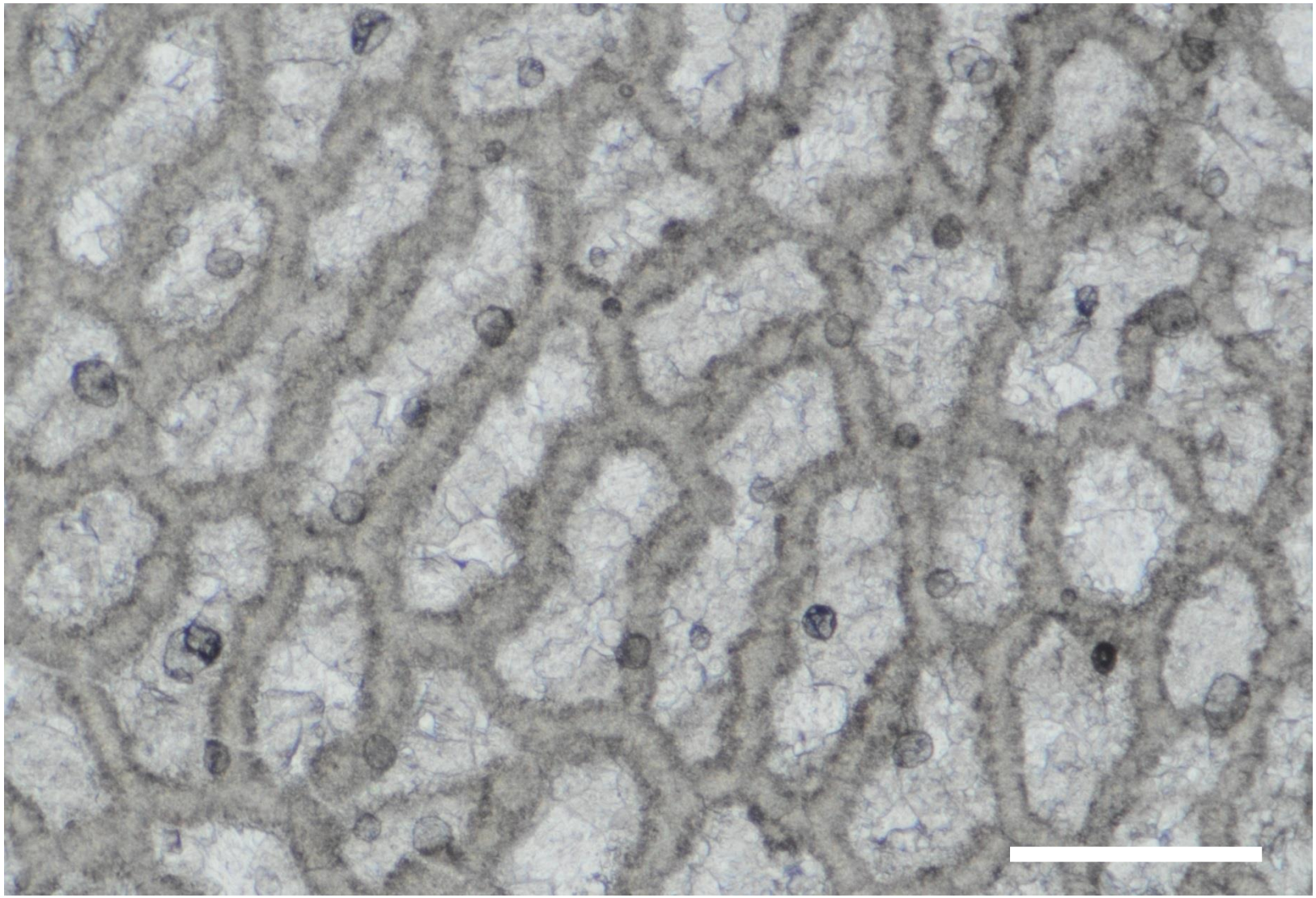

Figure 10. Thin section B6.3c showing walled calcispheres (the dark-rimmed circles) present on *Chaetetes*. Scale: 1 mm.

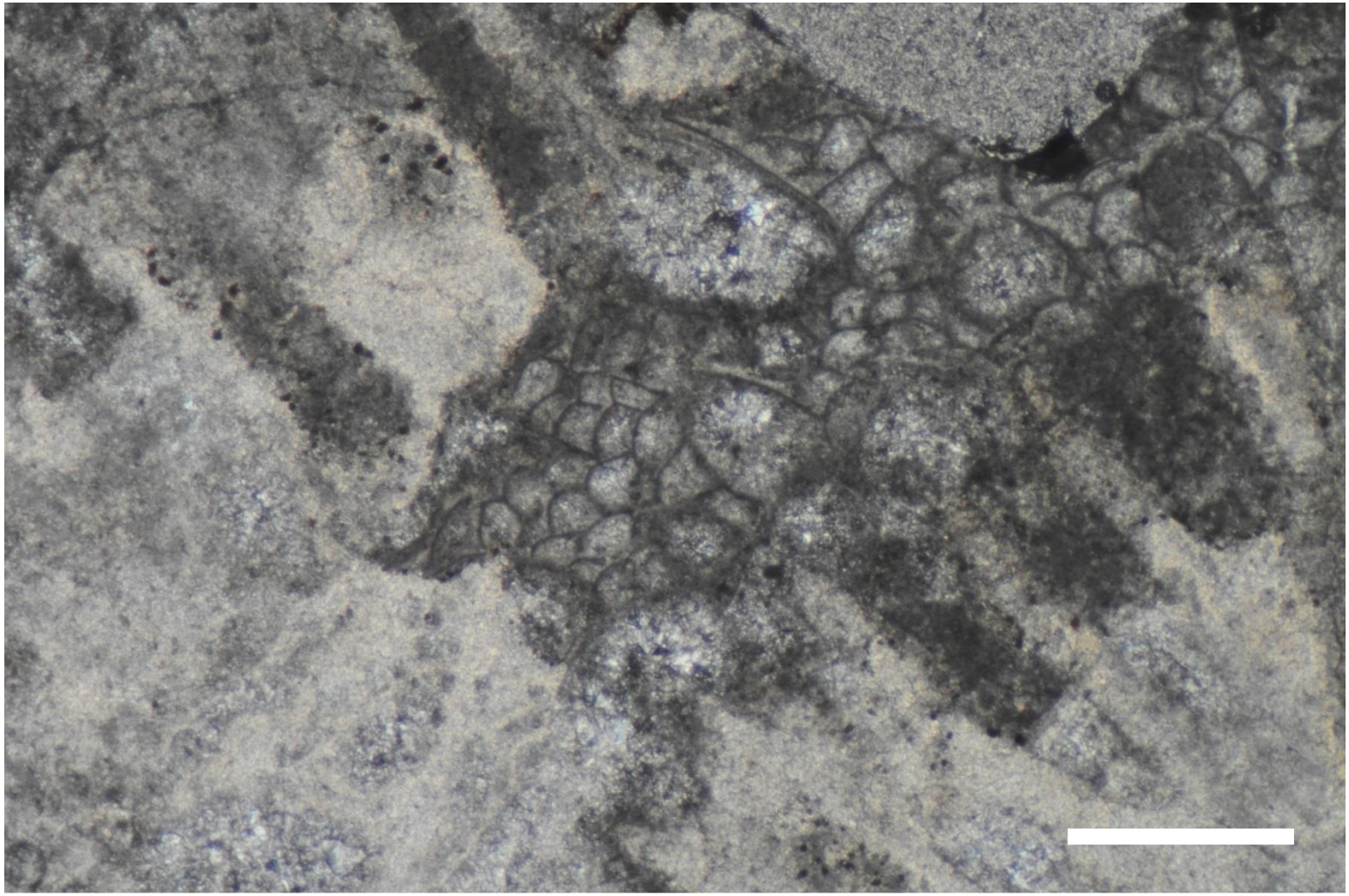

Figure 11. Thin section B6.3d showing slight encrustation of *Chaetetes* by phylloid algae. *Chaetetes* persists and grows over top of the phylloid algae (up is to the upper left). Scale: 1 mm.

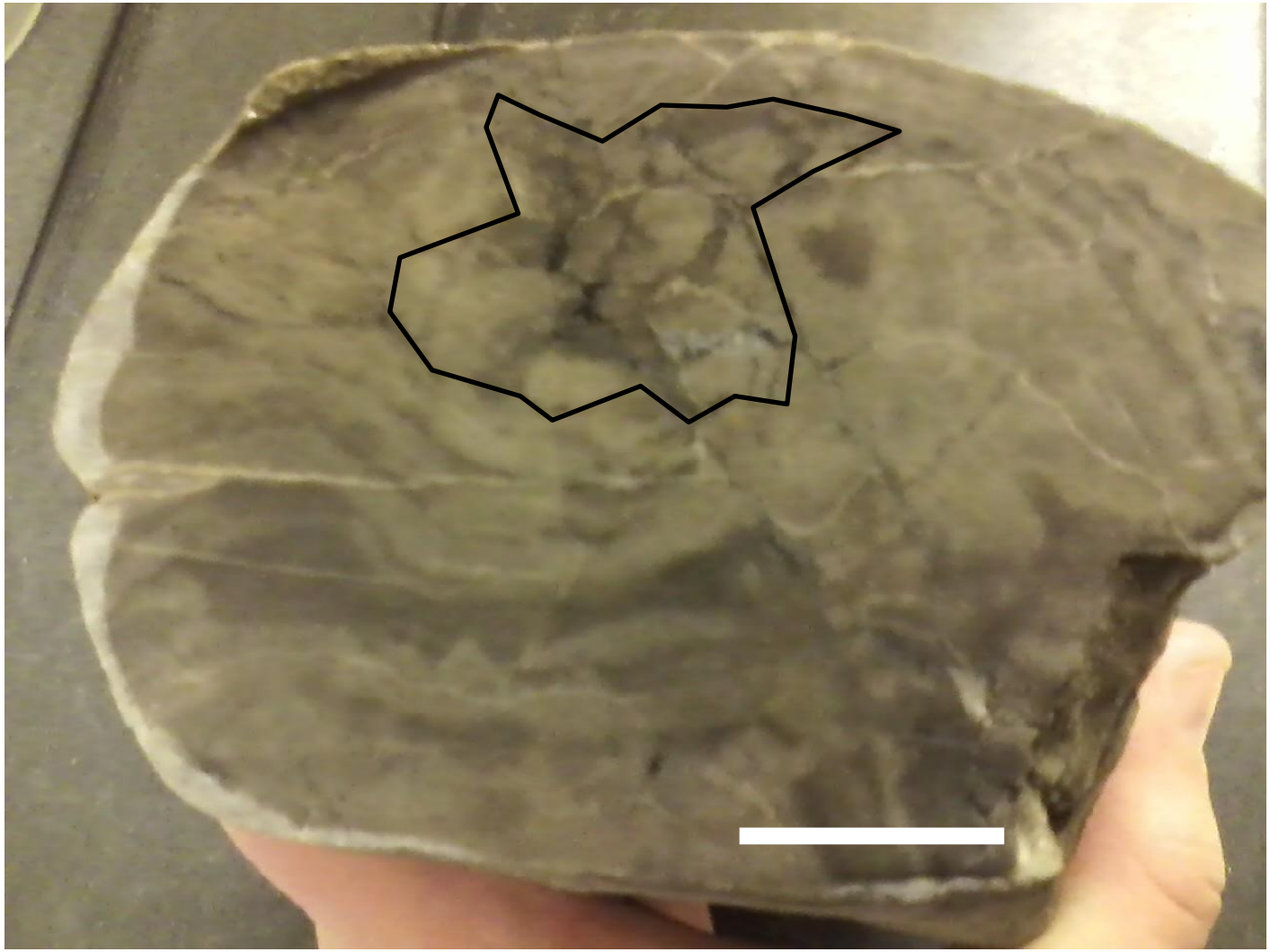

Figure 12. Hand sample T1.1 showing two distinct growth directions, outlined by a black line here for clarity. Within the black line the sponge appears to have grown laterally (across the surface), outside of the black line the sponge appears to have grown vertically (into the picture, in this case). Scale: 2 cm

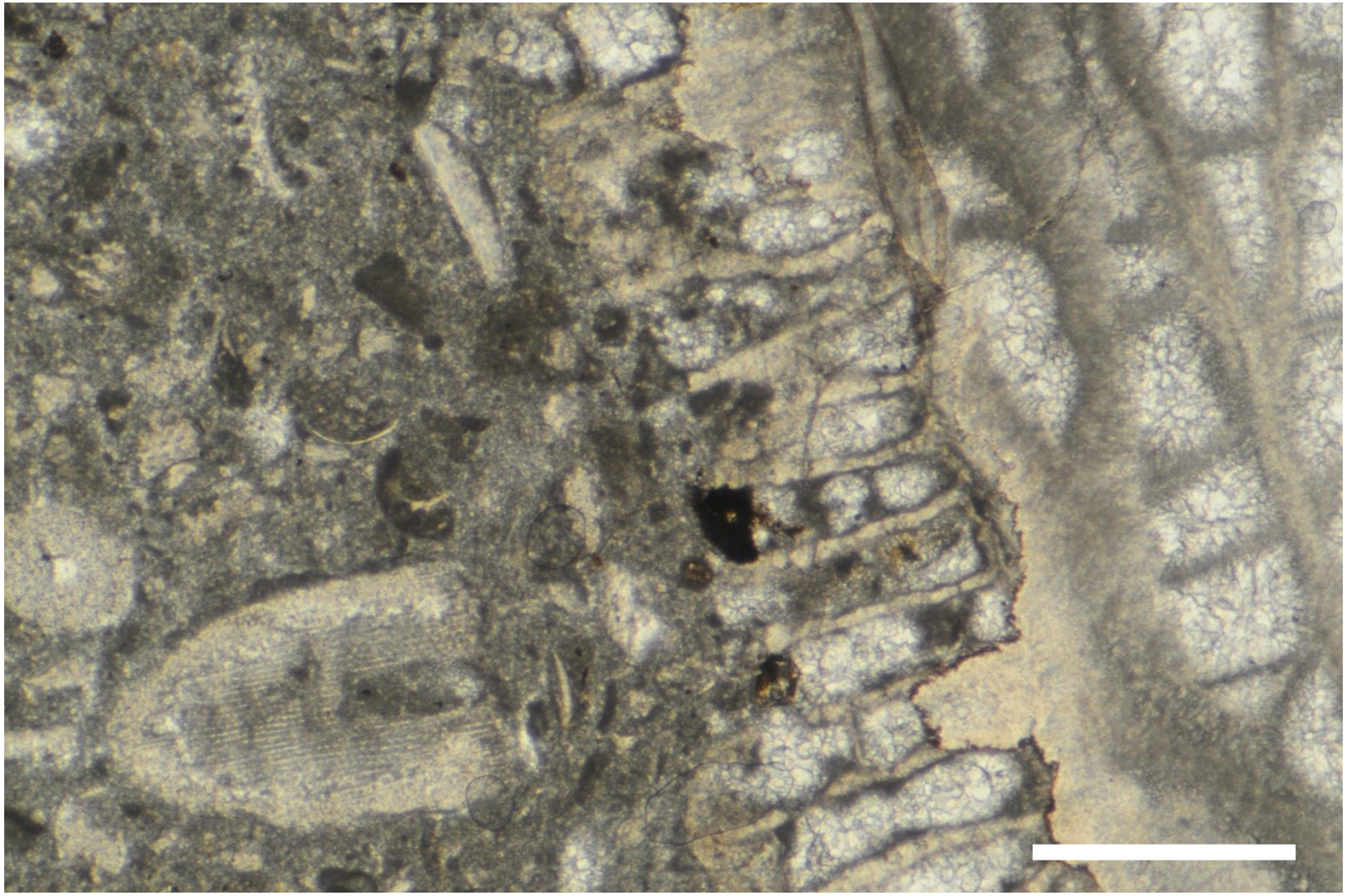

Figure 13. Thin section B1.1b1 showing two distinct growth directions of a single chaetetid sponge divided by a vertical line of iron staining. Scale: 1mm.

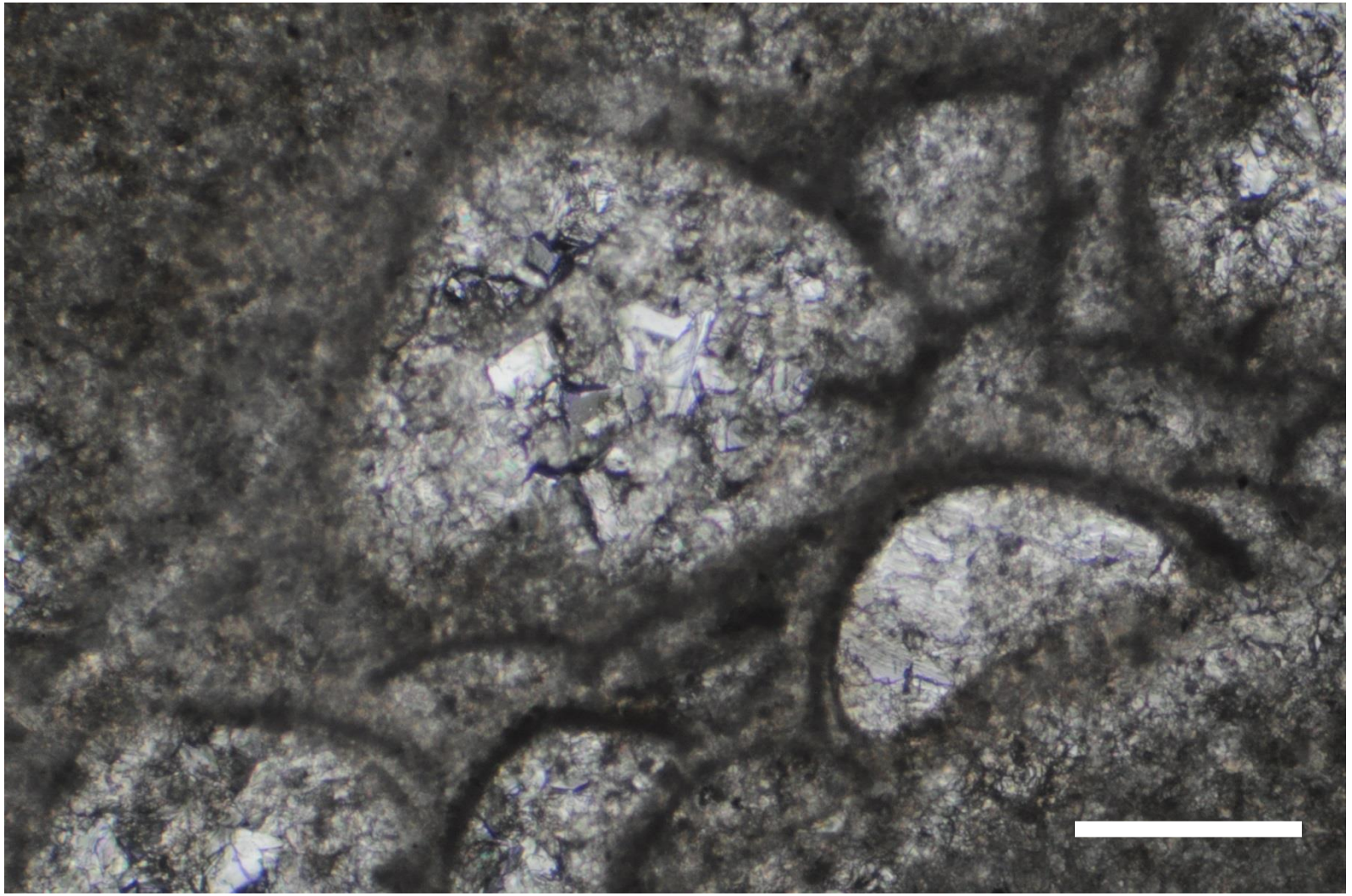

Figure 14. Thin section B6.3d showing phylloid algal texture and accompanying void space infilled with sparry calcite. Scale: 1mm.

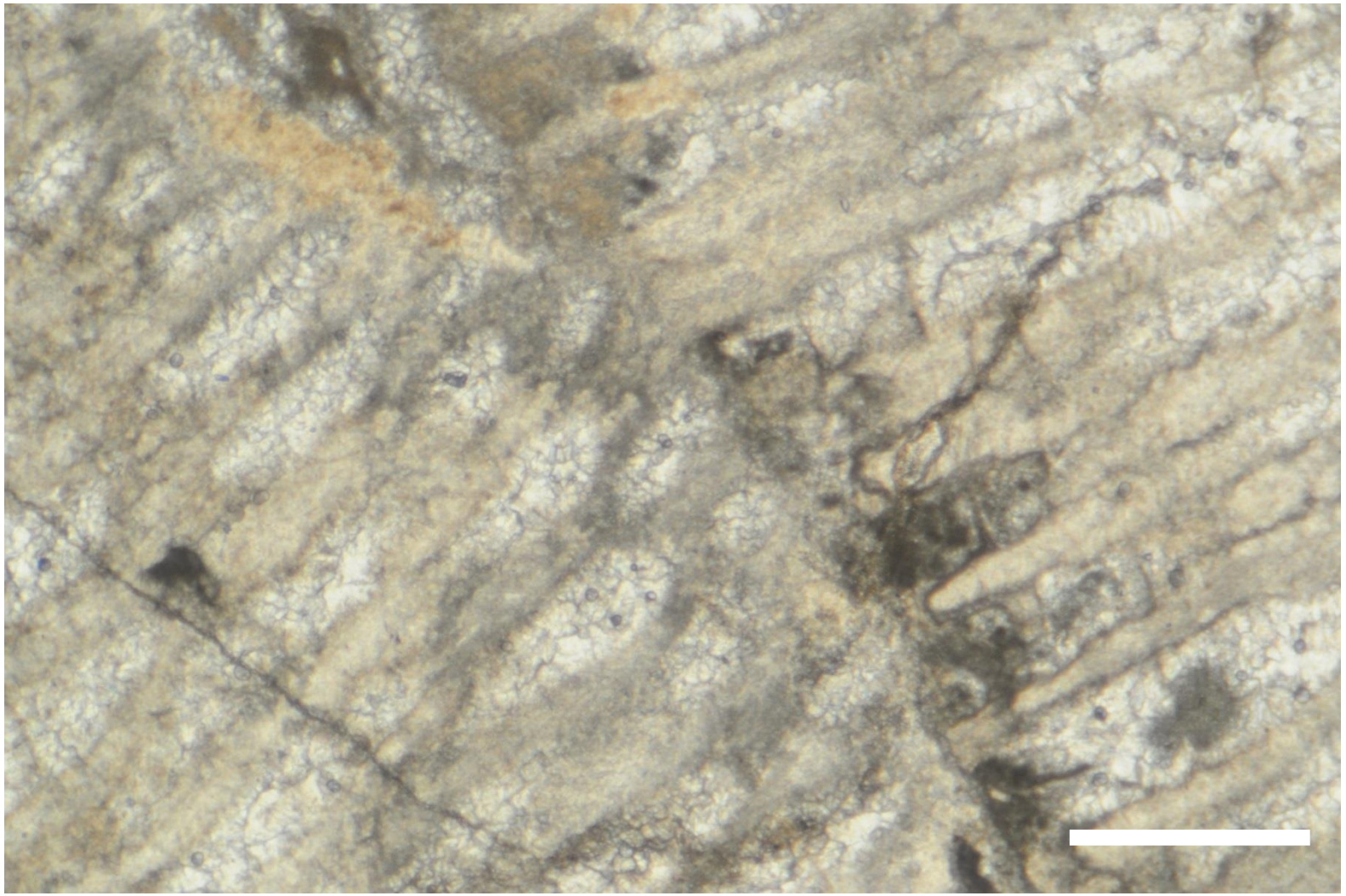

Figure 15. Thin section B1.1a2 showing two sponges growing against each other, possibly competing for growth space within the bioherm. Scale: 1mm

Appendix

Numbering System:

B/T before the number indicates original location in the laboratory where the samples were retrieved from, either a box or a tray. The number before the decimal point is the sample number. In cases where there were multiple samples per laboratory location, a decimal point and number were added after the sample number to indicate which specific sample was used. Lowercase letters following a decimal point indicate a labeled side of the sample, a number following this letter indicates how many thin sections were retrieved from each side. If there is not a number present after a lowercase letter then it indicates that the sample broke during cutting and resulted in multiple fragments of the original sample – each letter corresponds to a specific fragment.

For example:

B (box) **1** (sample #) **.1** (piece 1) **a** (side a) **1** (thin section 1)

T (Tray) **6** (sample number) **.a** (thin section of fragment a)

*Note: All scale bars on Figures are equivalent to 1 millimeter.

Sample Descriptions					
Figure Number*	Sample Location	Sample Number	Thin Section	Hand Sample Description	Thin Section Description
1	Molas Lake	B1.1	a1	Sponge sample preserving 2 sponges in growth position. Shape: curved wedge, height 20.2 cm width 15.6 cm. Crinoid fragments and shell fragments are visible.	Micrite sample showing crinoid fragments, shell fragments, foraminiferans, 1 ostracod half-shell, iron staining along boundaries, and veining throughout.
			a2		Two sponges present, showing boundary between the two where they appear to grow against each other. Possible walled calcispheres (but may also be water caught between the sample and the cover slip). Veining and iron staining present.

			b1		Sponge present, showing two distinct growth directions. Iron staining present along sponge-biomicrite boundaries, extensive veining throughout. Shell fragments, crinoid fragments, sponge fragments, foraminiferans present in the biomicrite.
			b2		Sponge present, showing iron staining. Extensive veining throughout, also with iron staining present along boundaries. Crinoid fragments, shell fragments and foraminiferans present in the biomicrite. Possible walled calcispheres (more likely water between the sample and the cover slip.
2	Molas Lahe	T2	a	Small disc of biomicrite. Approximately 8.5 cm in diameter and 2 cm in width. No clasts are readily identifiable.	Walled calcispheres, shell fragments, crinoids, parts of foraminiferans: everything is VERY broken and difficult to identify. Microveining and microfractures are present.
3	Molas Lake	B6.1a	N/A	One sponge, growing horizontal from left (connecting to 6.3) to the right at ~45° angle. Crinoids appear to have been overgrown here as well. The infill that the sponge is sitting on has visible crinoid fragments and shell fragments as well. Veins present throughout. Iron staining present along edges of sponge and near crinoid fragments within. Differences in infill texture: two lobes with significantly more fragments visible within the infill: center and bottom right corner. Hand sample shape: cone-minus-point (almost) Left width: 8.17cm. Center width: 7.26cm. Right width: 3.88cm. Length: 10.07cm.	N/A

		B6.1b	N/A	~2" of material was taken out from between 6.1a and 6.1b during the cutting process. Sponge growth is subhoriztonal at ~10° angle. Crinoid pieces present within the sponge in greater abundance on this side - also more clustered near areas where the sponge fractured and veined. Iron staining is present along fracture lines, within the infill and sponge cavities - also coats some crinoid stalk pieces. Iron staining shows elongated cavities within the sponge, suggesting extension of the original dimensions of the sponge. Infill above and below the sponge are the same composition in approximately the same ratios (foraminiferans, shell and crinoid fragments).	N/A
		B6.2	e	One sponge, interrupted by/ wrapping around infill. Crinoids visible, as well as iron staining along veins and fractures, as well as within sponge cavities. Hand Sample Shape: bulging cylinder. Hand Sample Size: Length:	Present: foraminiferans, crinoids, shell fragments, some iron staining. Possible Phylloid algal grains (45 microns long, 10 microns thick: largest). Micro-veins throughout specimen.

			g	10.09cm. Widest width: 10.35cm. Left end width: 5.03cm. Right end width: 6.92cm. (This hand sample sits perpendicular to 6.4 and 6.3 - connecting the two)	Sponge present in sample, in two pieces. Foraminiferans present. Shell fragments/ crinoids present. Walled calcispheres and unwalled calcispheres present - walled (possible algal origins) unwalled (non-algal origins). Largest crinoid fragment: half-disk ~17 microns long, ~14 microns wide. Iron staining along fracture boundaries & across grains - a few instances where it coats grains completely. Slight scalloping within staining...not seen in other samples, possible remnant of previous material? Or just depositional texture? Crystal -filled cavities within the sponge along growth surfaces.
		B6.3	b	One sponge, two sections separated by ~1.42cm of infill. Left section (from 6.2 side) has a large crinoid stalk piece at the bottom right corner (outer diameter: 10.1 mm, inner diameter: 1.0 mm) - pressure solution evident on this piece. Iron staining present along sponge edges and within the infill material. Crinoid stem pieces present throughout the sponge - smallest visible: 0.1 mm - they look as if they dropped on top of the sponge as it was growing and were then overgrown by the sponge.	Predominantly sponge sample, slight biomicrite at bottom edge of slide - including foraminiferans and shell fragments. Iron staining is present around the edges of the sponge. Walled calcispheres are present across the sponge, but appear grouped in a few seemingly random places - perhaps nearer to the outside of the sponge - location of samples will need to be marked to better determine/ decide if there is a reason for the grouping of calcispheres in specific locations (no locational affinity was detected).
			c		Shell fragments, foraminiferans, crinoids, walled calcispheres and sponge fragments are present. Some matrix grains are unidentifiable (i.e. shell, algal grains, foraminiferans) - due to deformation/ cut angle through them.

			d		Unwalled calcispheres, crinoids, foraminiferans, and sponge fragments present. Within/ on top of sponge fragments: walled calcispheres, some iron staining around the edges, sparry calcite between 'growth rings' present...calcite has an odd texture - almost scalloped - within these.
			g		Biomicrite: foraminiferans, shell fragments, veining, whole shells (appear to be ostracods and very small clam-like shells), possible rip-up clasts (maybe just odd-colored sediment), iron staining present along vein edges and along the edges of/ across some shell fragments.
		B6.4	a	Large crinoid (6.2 x 4.6mm) and shell fragments (6.9 x 1.6mm). Side/ top of side of sponge. Veining present throughout, iron staining visible on sponge surface and on veins. Hand sample shape: narrowing rectangle. Hand sample size: Whole side length: 12.8 cm. Largest side width: 6.58 cm. Smallest side width: 3.24 cm.	Biomicrite: walled calcispheres, foraminiferans, crinoids, shell fragments, whole shells. Sponge fragment.
			b		Sponge: some veining, some iron staining (along veins and edges of sponge). Shell fragments in sparite in-fill, microveining.
4	Molas Lake	T6	a	Solitary sponge, with biomicrite present beneath it (~2 cm long, 3 cm thick) with visible crinoid and shell fragments	Sponge present in sample in a single piece (upper portion of the thin section), edges appear scalloped in places where it meets the biomicrite. Also present are shell fragments, one complete half-shell, crinoid fragments and foraminiferans.
5	Andrews Lake	T1.1	a	Vertical sponge growth, fracture patter may be evidence of rotational growth (algal growth	Sponge sample - microfractures and microveins present. Some iron staining along fractures.

			b	along no-longer active growth surfaces?) especially because this is the base of a single sponge. Hand Sample Shape: Ellipsoidal Hemisphere. Hand sample size: Long axis: 10.16 cm. Short axis: 6.97 cm.	Sponge sample - microfractures and microveins. Some iron staining along fractures.
6	Andrews Lake	B4	b	Curl-up clasts, rather than rip-up clasts, present - hence lobed appearance of clasts. Lighter colored areas: fragments are relatively more damaged; debris would be solid (though not lithified) prior to curling up. Darker colored areas: fragments are relatively less damaged; debris would be soft, but pliable, prior to curling up. Evidence to look for: boring structures/ drag marks/ pressure solution. Hand Sample Shape: Rectangle. Hand Sample size: Length: 3.41cm. Width: 2.93 cm.	Iron staining present throughout, coating grains and on edges of veins/ fractures. VERY broken fragments of shells, crinoids and foraminiferans. Curl-up clasts: the hand sample shows lobes of lighter and darker colored biomicrite. Identification of fragments is easier in darker colored lobes because the fragments are less broken and less deformed than in the lighter lobes.

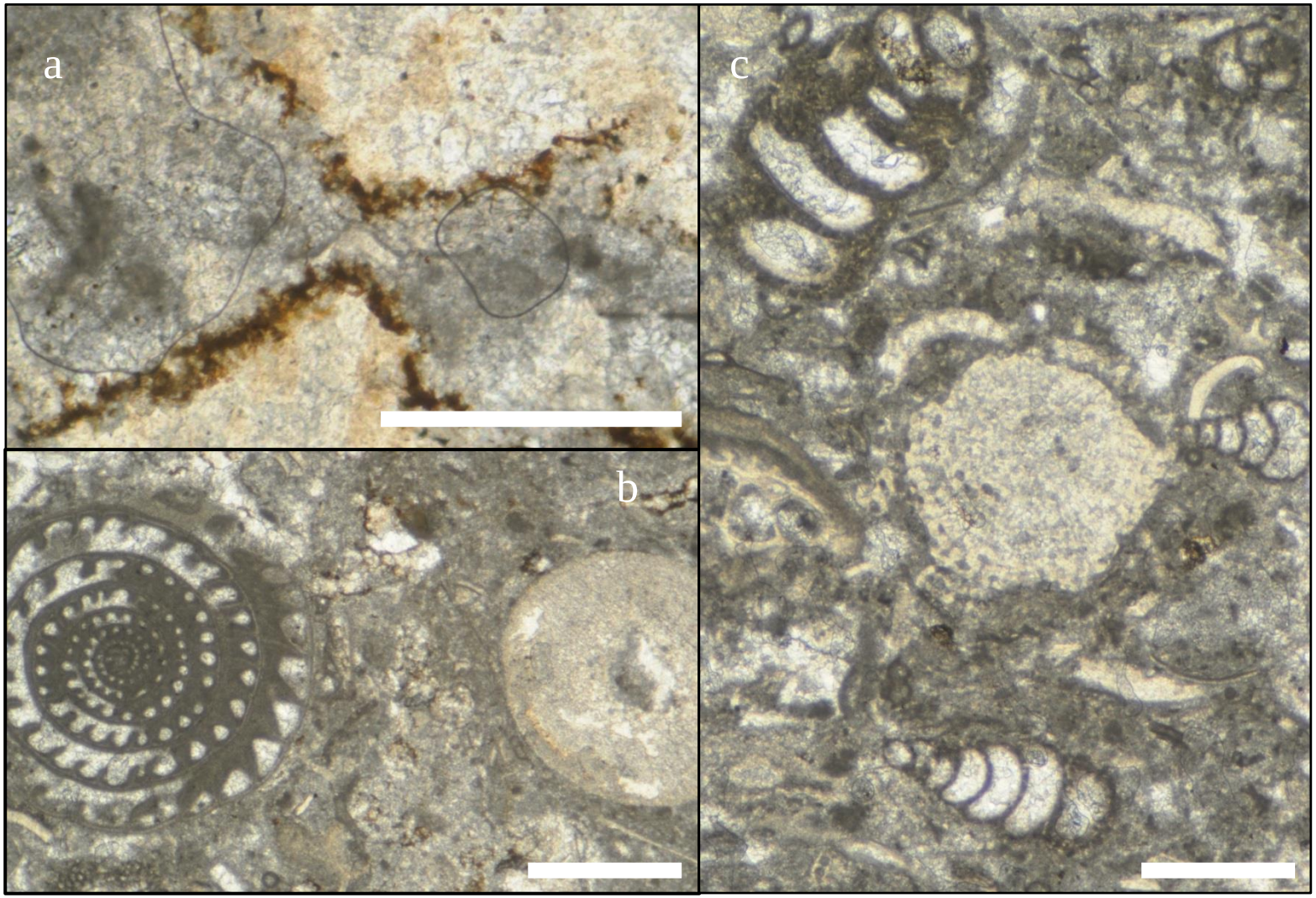

Figure 1. B1.1a1 a) Micrographs showing sponge/biosparite boundary and iron staining b) A foraminiferan and a crinoid stem fragment c) Foraminiferans, shell fragments and sponge fragments.

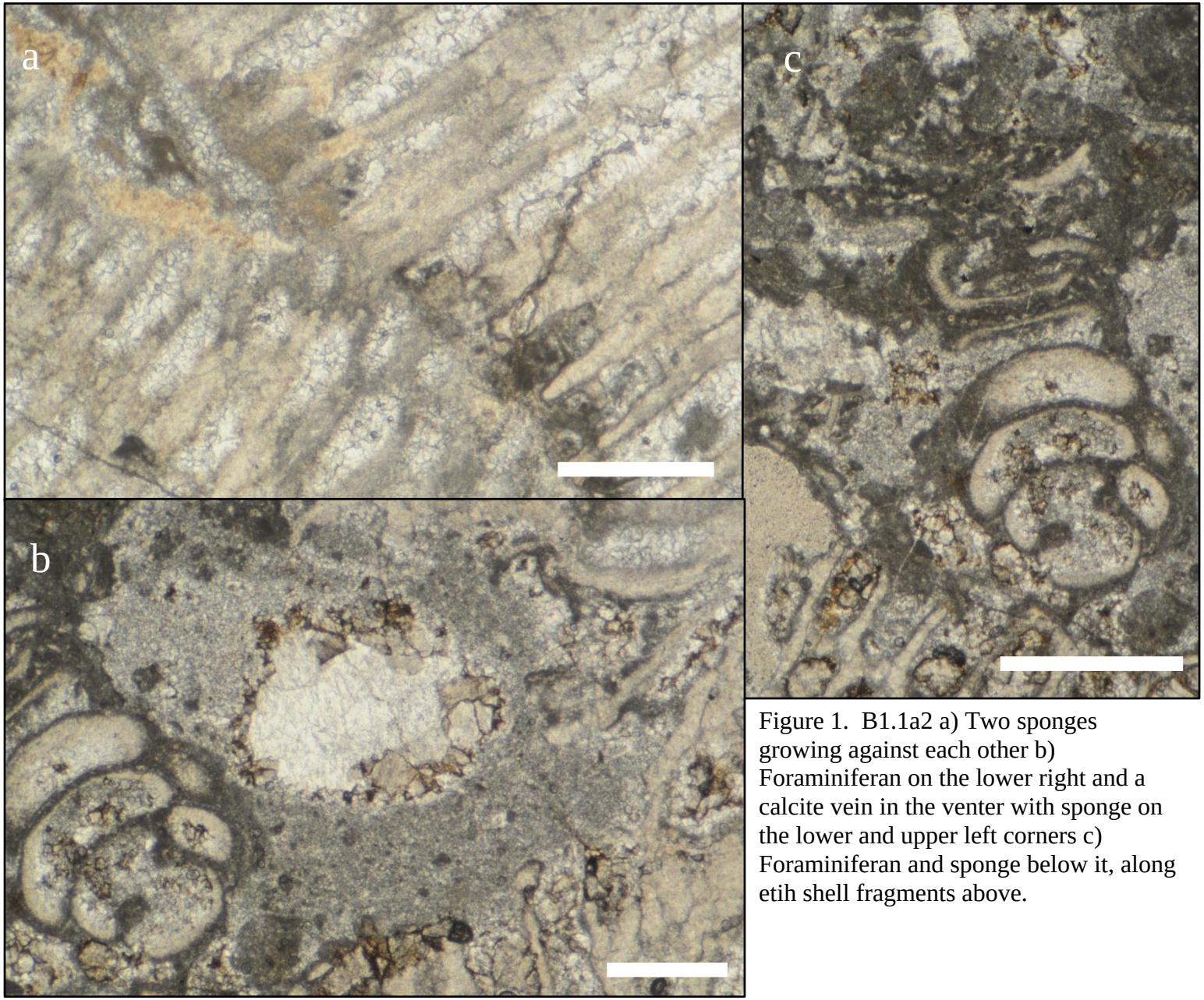

Figure 1. B1.1a2 a) Two sponges growing against each other b) Foraminiferan on the lower right and a calcite vein in the venter with sponge on the lower and upper left corners c) Foraminiferan and sponge below it, along etih shell fragments above.

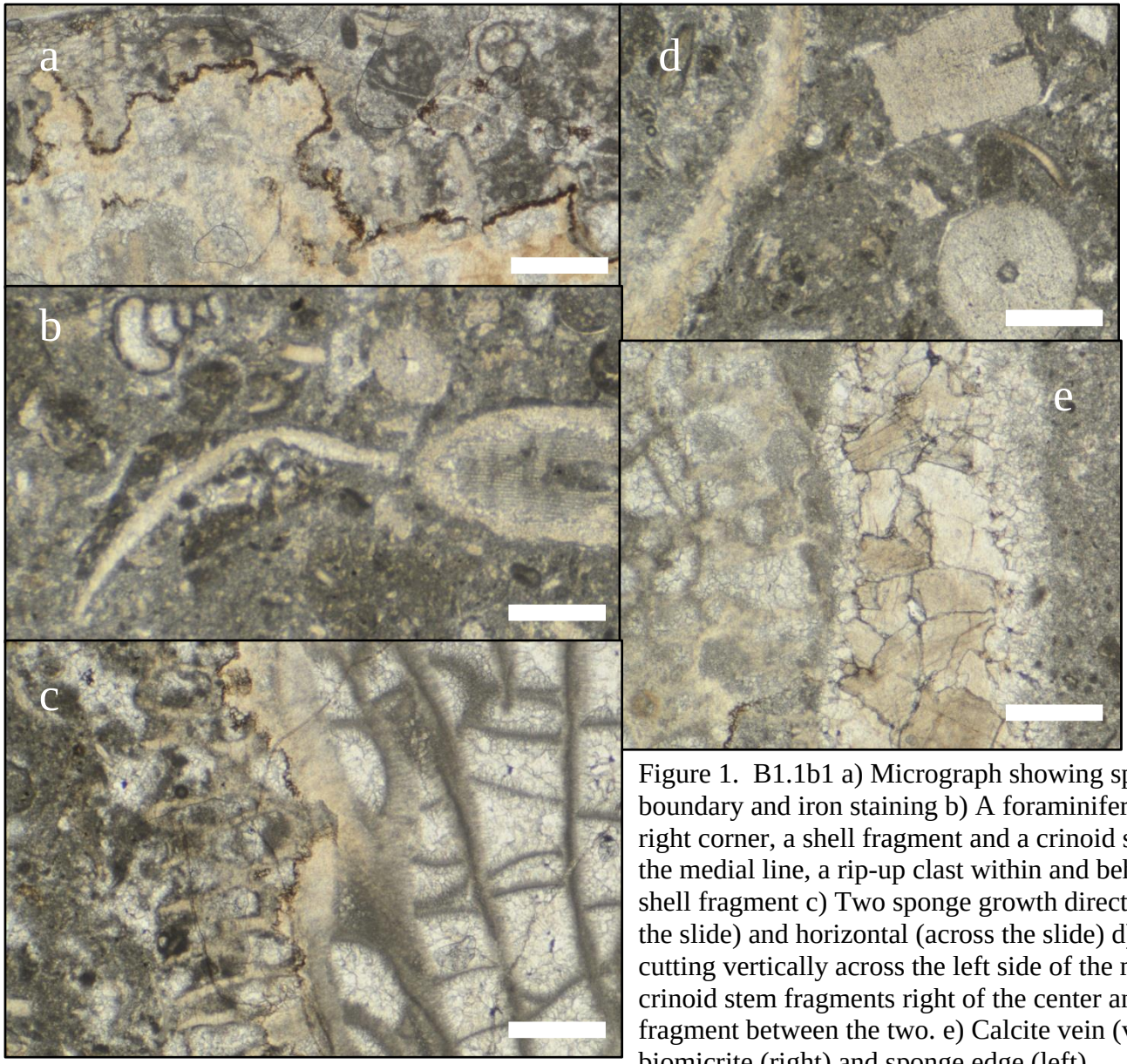

Figure 1. B1.1b1 a) Micrograph showing sponge/biosparite boundary and iron staining b) A foraminiferan in the upper right corner, a shell fragment and a crinoid stem fragment on the medial line, a rip-up clast within and behind the central shell fragment c) Two sponge growth directions vertical (into the slide) and horizontal (across the slide) d) shell fragment cutting vertically across the left side of the micrograph, two crinoid stem fragments right of the center and a shell fragment between the two. e) Calcite vein (venter) with biomicrite (right) and sponge edge (left)

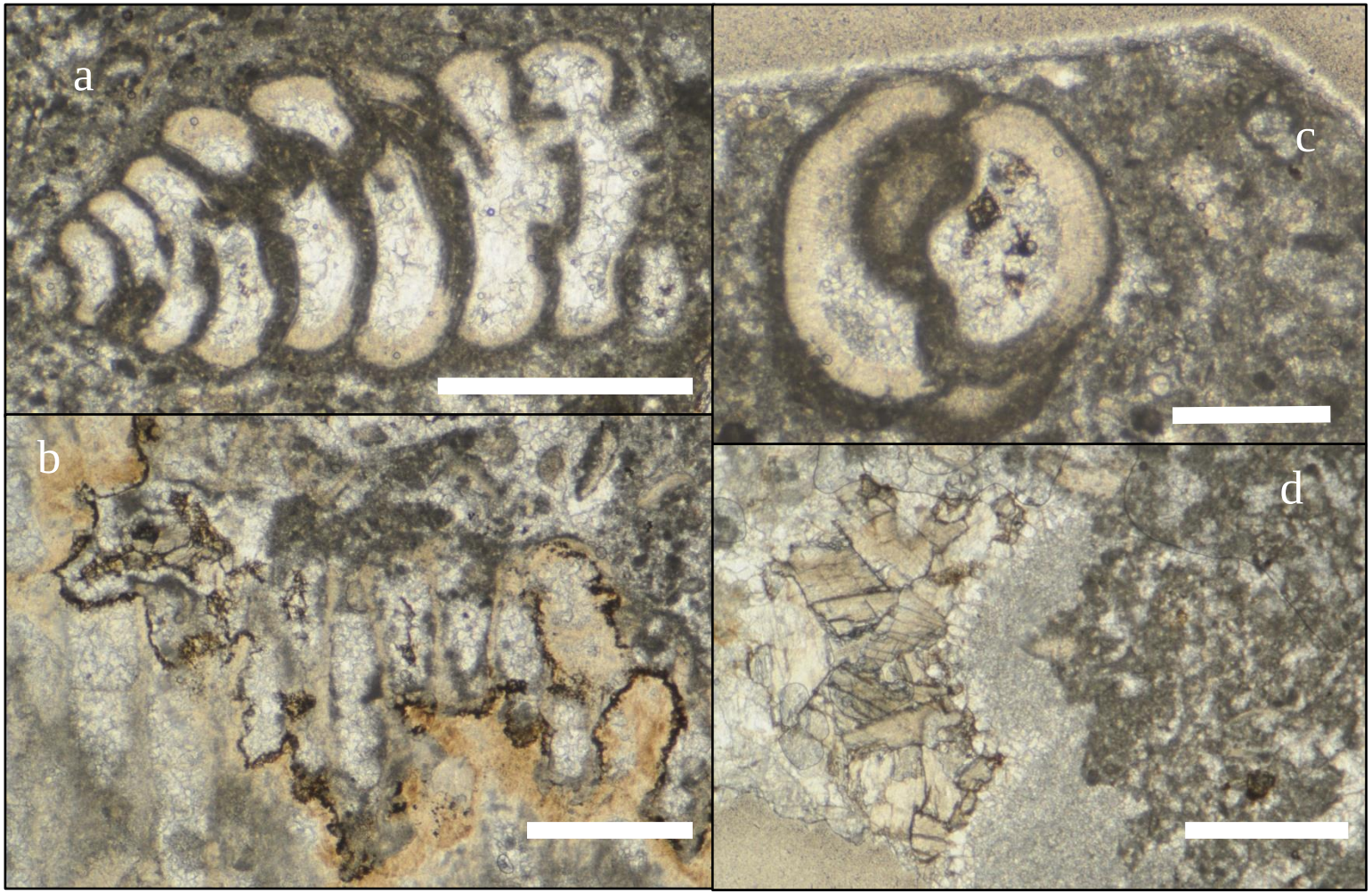

Figure 1. B1.1b2 a) Micrograph of a single, large fusilinid foraminiferan b) Sponge/biosparite boundary and iron staining, some calcite veining on the left, beside the sponge, and shell fragments above on the right c) A single fusilinid foraminiferan d) a calcite vein on the left half of the slide and a biosparite on the right.

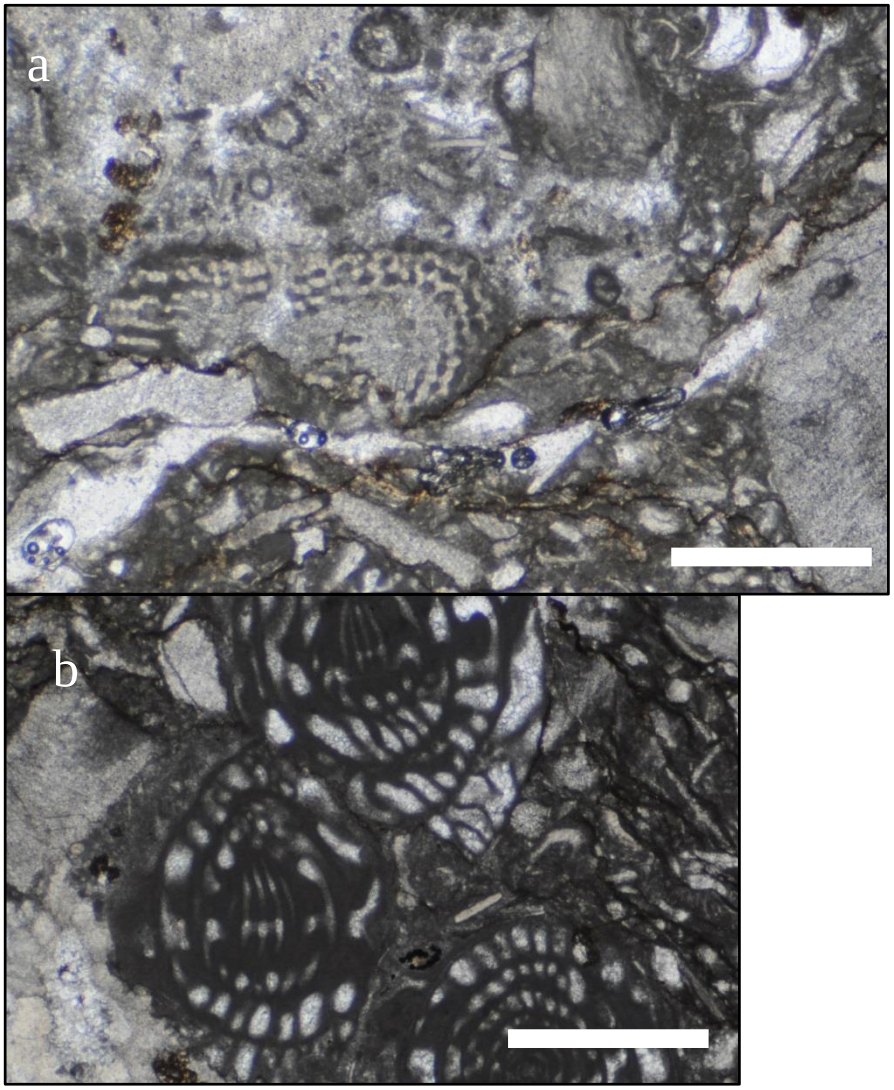

Figure 2. T2.e a) Micrograph showing biosparite containing a sponge fragment (center), and shell and crinoid stem fragments throughout b) Three closely-spaced foraminiferans in biosparite.

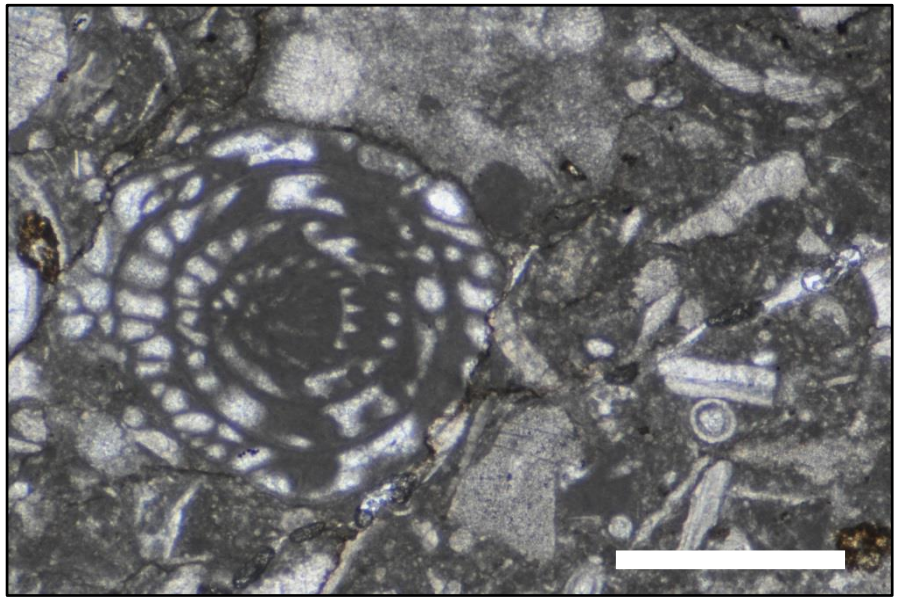

Figure 3. B6.2e Micrograph showing a foraminiferan (left center) and various shell and crinoid stem fragments surrounding it.

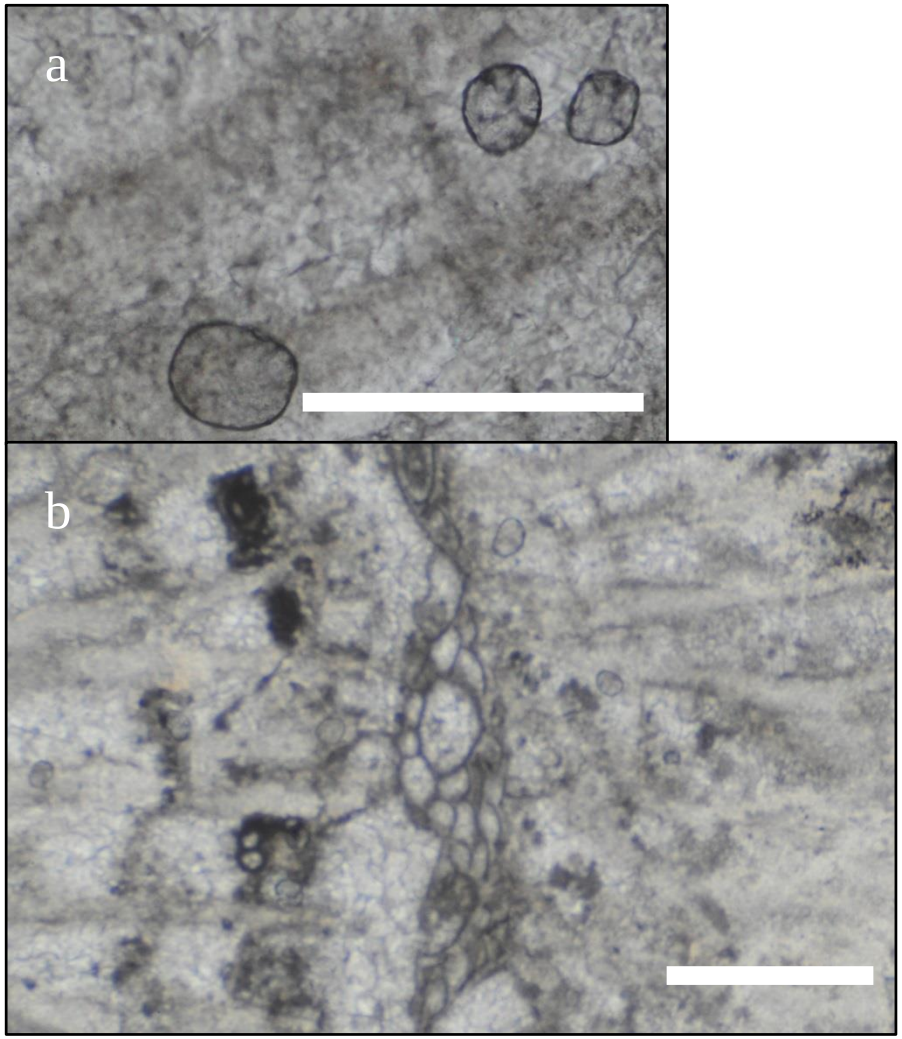

Figure 3. B6.2g a) Micrograph showing walled calcispheres on *Chaetetes* b) Phylloid algae between sponge growth surfaces.

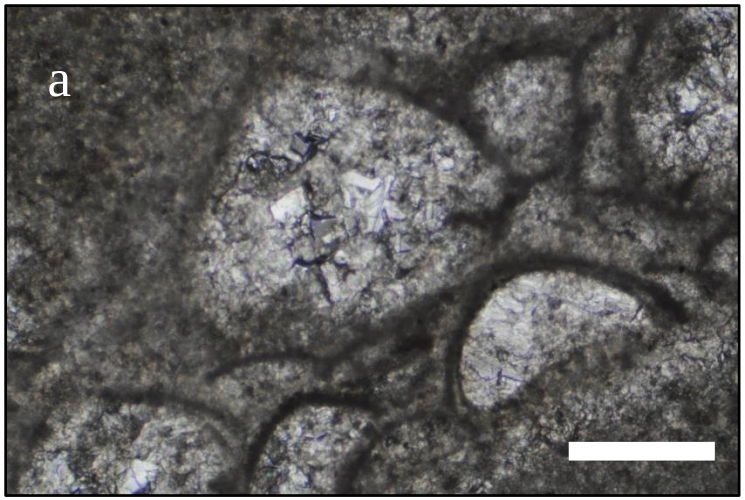

Figure 3. B6.3b a) Micrograph showing phylloid algal texture.

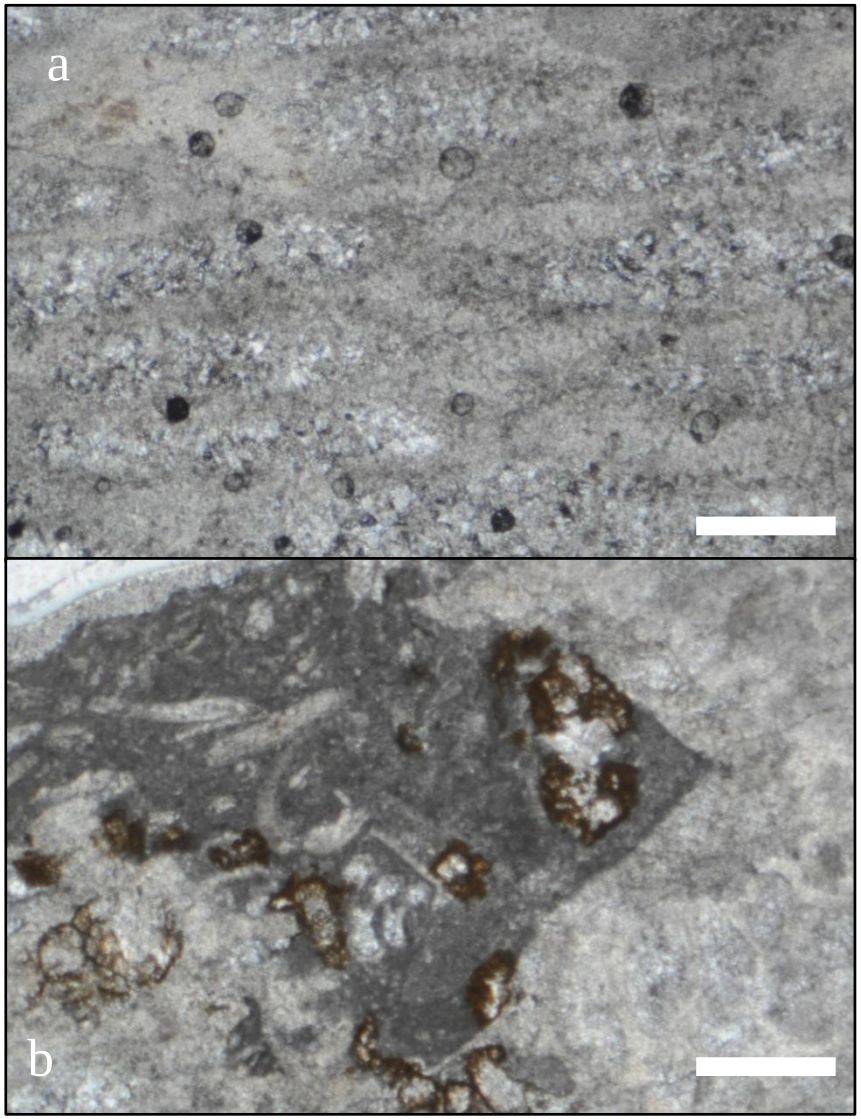

Figure 3. B6.3c a) Micrograph showing walled calcispheres and coated calcispheres on the surface of *Chatetes* b) Sponge/biosparite boundary with iron staining coating clast fragments within the biosparite.

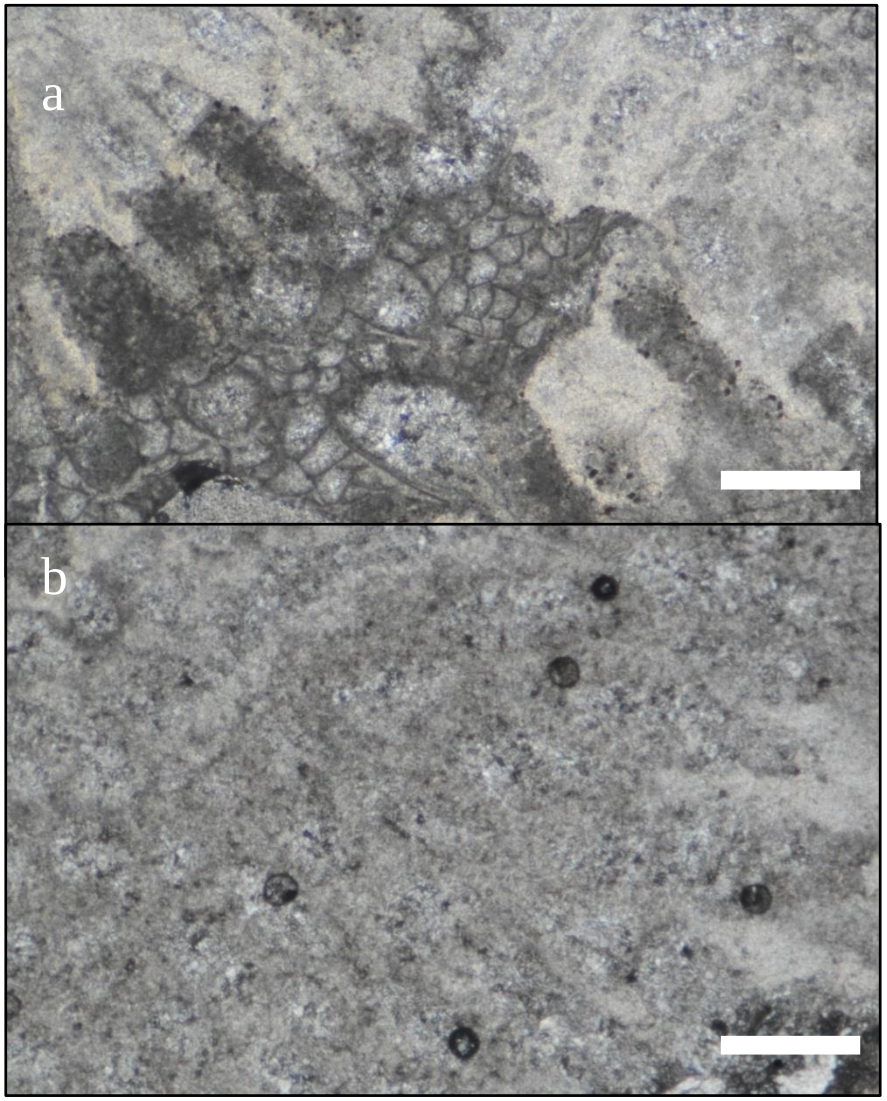

Figure 3. B6.3d a) Micrograph showing phylloid algal texture between sponge growth surfaces b) Coated calcispheres on *Chaetetes*.

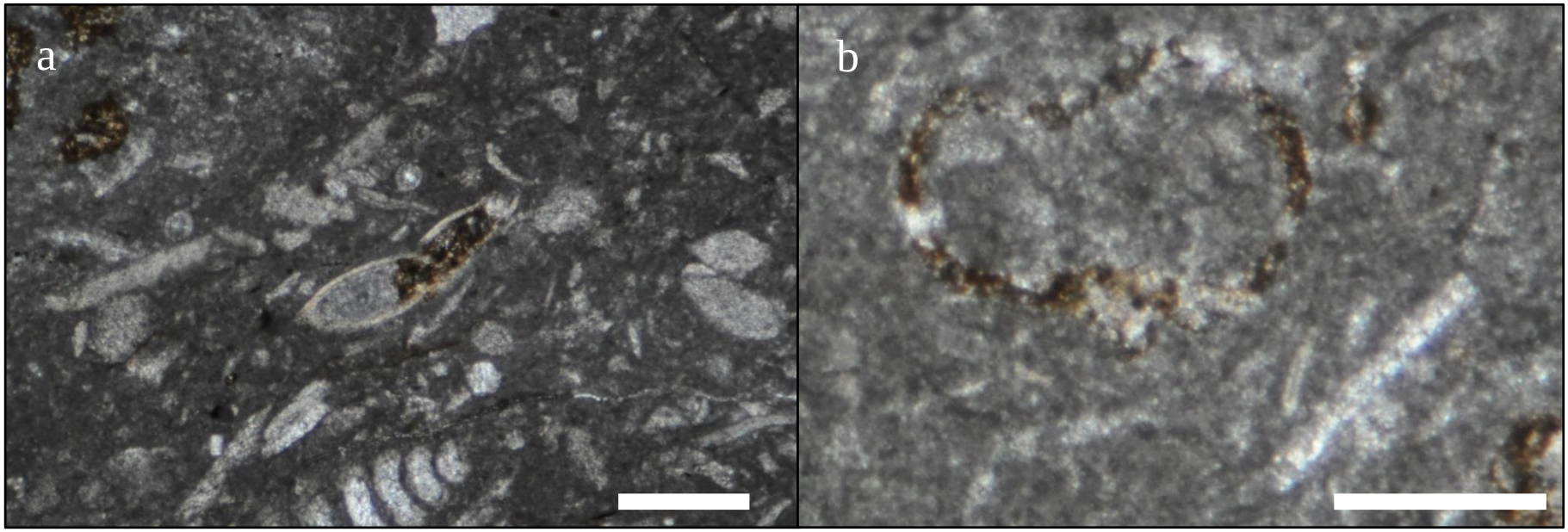

Figure 3. B6.3g a) Micrographs showing biosparite with complete open shell (iron staining within half of the shell), foraminiferan at the bottom, and shell and crinoid fragments throughout. b) B6.4a A complete shell-outline in iron staining in the center and shell fragments to the right of it.

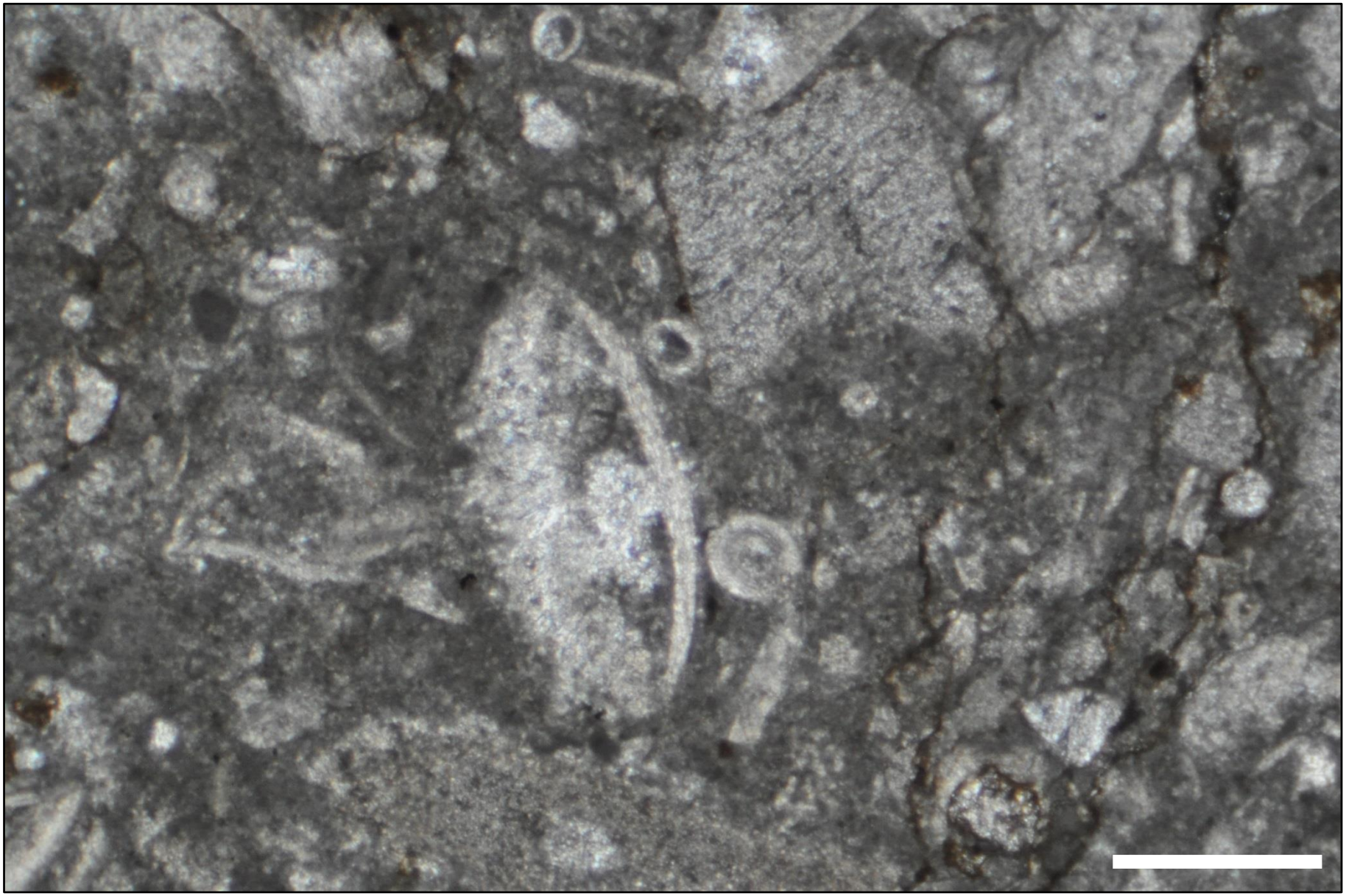

Figure 3. B6.4b Micrograph showing a complete, close shell (center) crinoid stem fragments and shell fragments throughout.

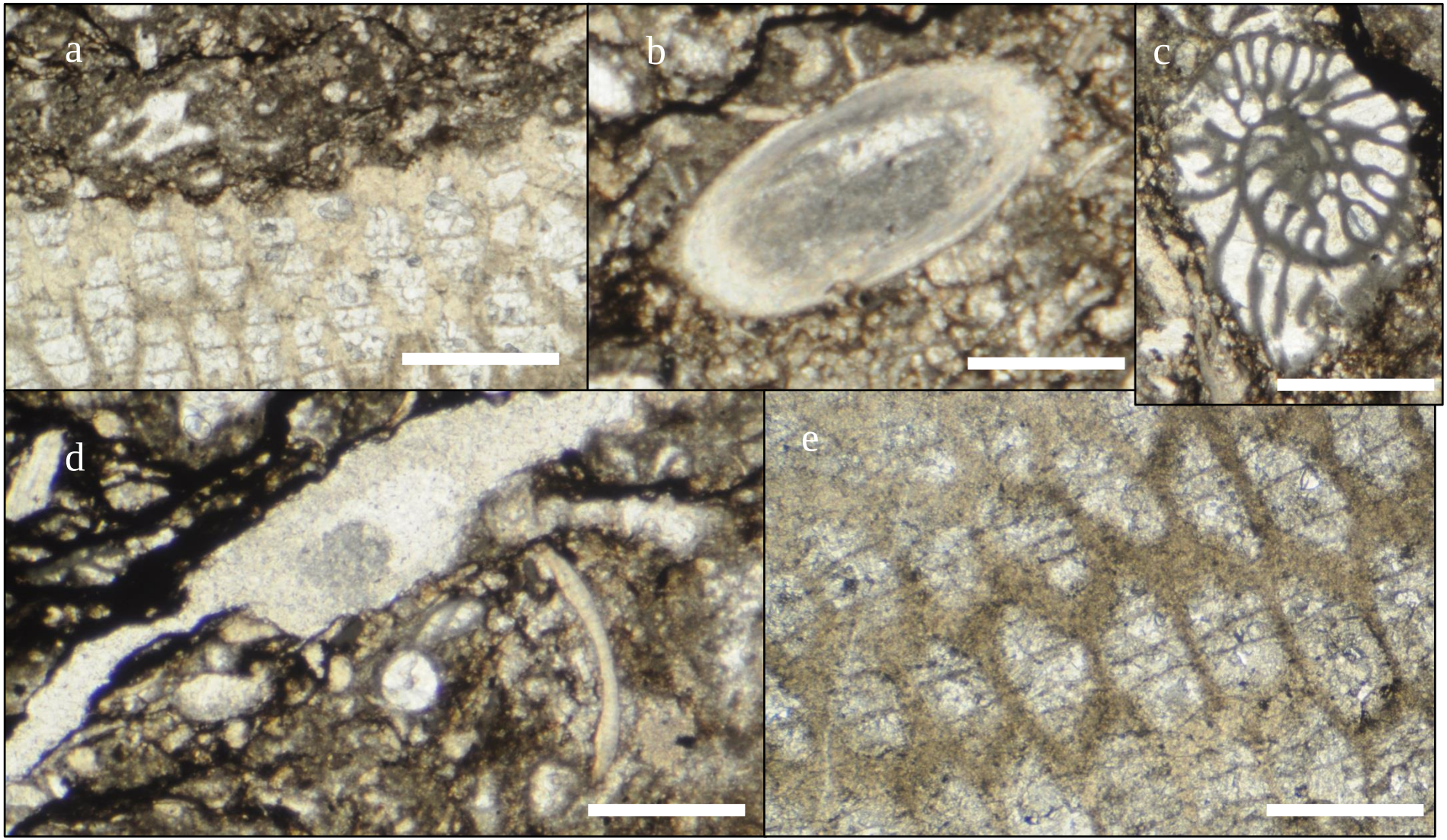

Figure 4. T6.a a) Micrographs showing sponge/biosparite boundary b) a partial ostracod shell c) a foraminiferan d) crinoid and shell fragments (large white space is a crack in the sample) e) *Chaetetes* growth habit.

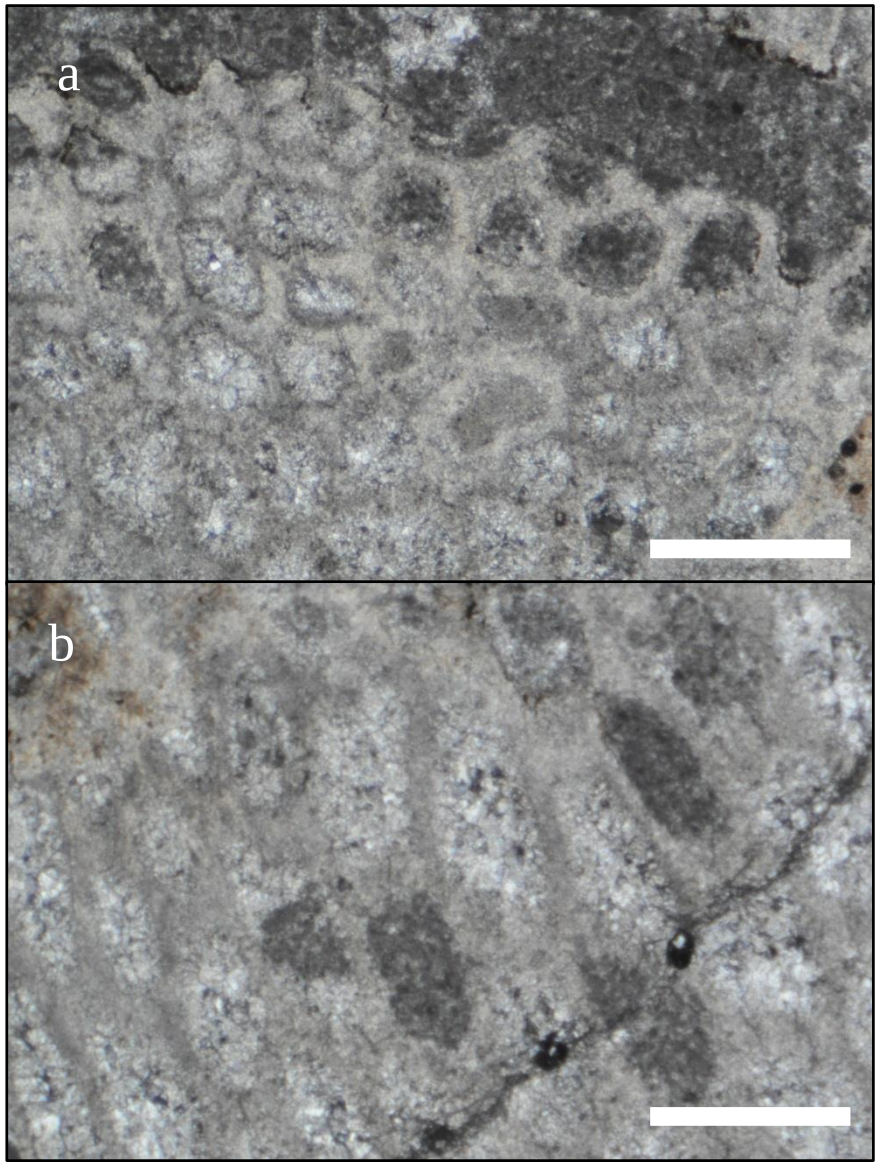

Figure 5. T1.1a a) Micrographs showing sponge/biosparite boundary b) Sponge growth habit and a microvein

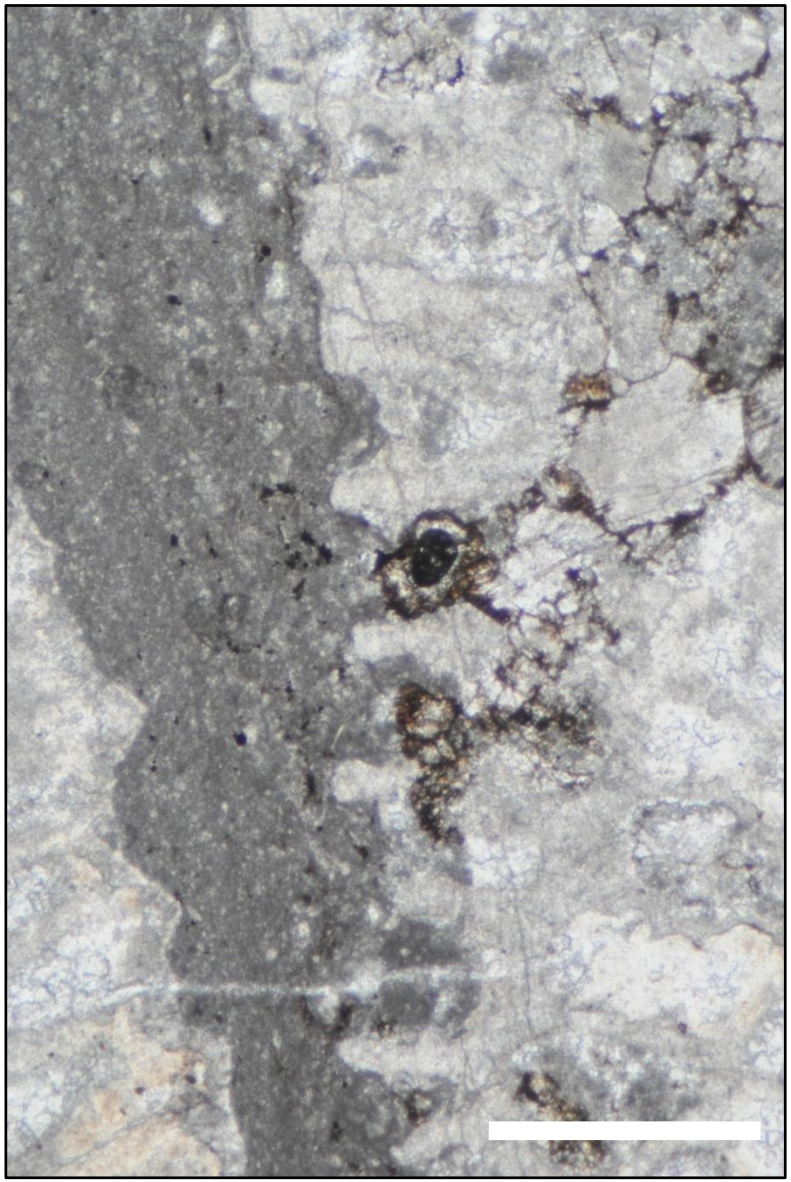

Figure 5. T1.1b Micrograph showing sponge on the left, biosparite in the middle and a calcite vein on the right with some iron staining.

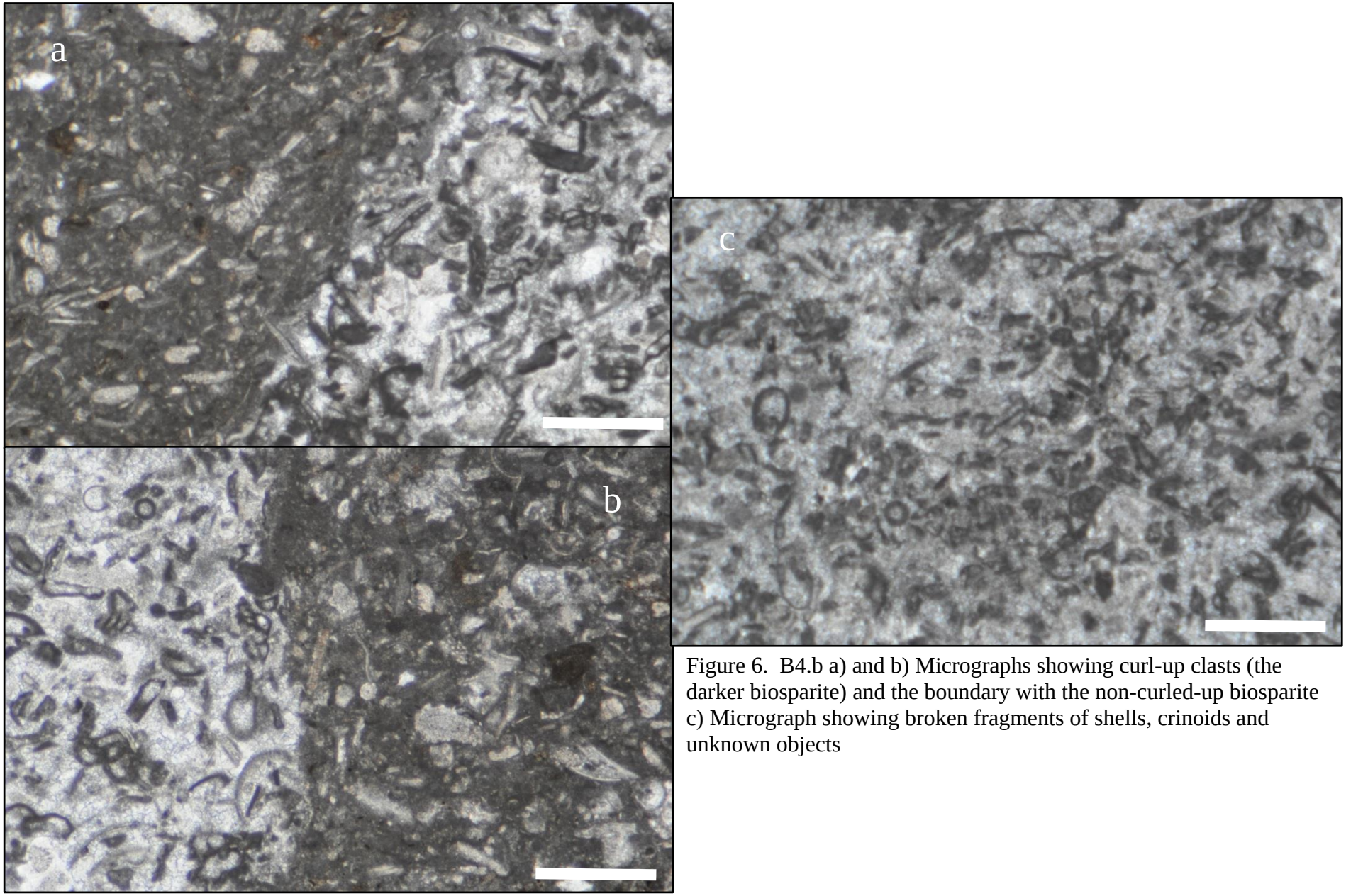

Figure 6. B4.b a) and b) Micrographs showing curl-up clasts (the darker biosparite) and the boundary with the non-curled-up biosparite c) Micrograph showing broken fragments of shells, crinoids and unknown objects